

## Multiparameter Critical Situations, Universality and Scaling in Two-Dimensional Period-Doubling Maps

S. P. Kuznetsov,<sup>1,2</sup> A. P. Kuznetsov,<sup>1,2</sup> and I. R. Sataev<sup>1</sup>

*Received January 11, 2005; accepted May 20, 2005*

---

We review critical situations, linked with period-doubling transition to chaos, which require using at least two-dimensional maps as models representing the universality classes. Each of them corresponds to a saddle solution of the two-dimensional generalization of Feigenbaum-Cvitanović equation and is characterized by a set of distinct universal constants analogous to Feigenbaum's  $\alpha$  and  $\delta$ . One type of criticality designated H was discovered by several authors in 80-th in the context of period doubling in conservative dynamics, but occurs as well in dissipative dynamics, as a phenomenon of codimension 2. Second is bicritical behavior, which takes place in systems allowing decomposition onto two dissipative period-doubling subsystems, each of which is brought by parameter tuning onto a threshold of chaos. Types of criticality designated as FQ and C occur in non-invertible two-dimensional maps. We present and discuss a number of realistic systems manifesting those types of critical behavior and point out some relevant conditions of their potential observation in physical systems. In particular, we indicate a possibility for realization of the H type criticality without vanishing dissipation, but with its compensation in a self-oscillatory system. Next, we present a number of examples (coupled Hénon-like maps, coupled driven oscillators, coupled chaotic self-oscillators), which manifest bicritical behavior. For FQ-type we indicate possibility to arrange it in non-symmetric systems of coupled period-doubling subsystems, e.g. in Hénon-like maps and in Chua's circuits. For C-type we present examples of its appearance in a driven Rössler oscillator at the period-doubling accumulation on the edge of synchronization tongue and in a model map with the Neimark-Sacker bifurcation.

---

**KEY WORDS:** Period-doubling; onset of chaos; renormalization group; universality; scaling; coupled maps; coupled oscillators; multi-parameter analysis.

---

<sup>1</sup>Institute of Radio-Engineering and Electronics of RAS, Zelenaya 38, Saratov, 410019, Russian Federation; e-mail: kuznetsov@sgu.ru

<sup>2</sup>Faculty of Nonlinear Processes, Saratov State University, Bolshaya Kazachya, 112A, Saratov, 410012, Russian Federation.

The paper is dedicated to the 60th birthday of Mitchel J. Feigenbaum

## 1. INTRODUCTION

An important aspect of the problem of turbulent dynamics in spatially extended systems of different nature is the question: how does the spatio-temporal chaos originate from simple regular regimes as we vary one or more control parameters?

The breakthrough in understanding the onset of chaos in low-dimensional systems was Feigenbaum's discovery of the period-doubling universality and the renormalization-group (RG) approach.<sup>(1,2)</sup> The one-dimensional non-invertible iterative maps represent the simplest class of systems, which exhibit the Feigenbaum type of behavior. However, the period-doubling transition to chaos with the same universal quantitative regularities occurs in many multi-dimensional dissipative nonlinear systems.<sup>(1-4)</sup> It takes place, for example, in the Lorenz and Rössler models,<sup>(5-7)</sup> in two-dimensional maps of Hénon and Ikeda,<sup>(8,9)</sup> in synchronized systems inside the Arnold tongues,<sup>(10)</sup> in periodically driven dissipative nonlinear oscillators,<sup>(11-14)</sup> in phase-locked loops,<sup>(15)</sup> in self-oscillating electronic systems, like Anishchenko – Astakhov oscillator,<sup>(16)</sup> Dmitriev – Kislov oscillator,<sup>(17)</sup> Chua circuit,<sup>(18)</sup> microwave backward-wave oscillator.<sup>(19)</sup> Experimental observations of the Feigenbaum scenario were reported in convection in liquid helium<sup>(20)</sup> and in mercury,<sup>(21)</sup> in acoustical oscillations of bubbles in fluid,<sup>(22)</sup> in Q-switched lasers,<sup>(23)</sup> in hybrid acoustic-optical systems with delay.<sup>(24)</sup> This list may be continued.

As long as the Feigenbaum theory is applicable for a multidimensional spatially extended system, it allows understanding the onset of regimes of only restricted complexity, of certain spatial forms, which are governed by dynamics of one variable in time described in terms of one-dimensional model maps.

When new modes consequently come into play in a course of parameter variation on a road to developed spatio-temporal chaos, effective dimension of the dynamics increases, and description in terms of the one-dimensional maps inevitably becomes insufficient. In this paper, we review several situations associated with period doubling, which require at least two-dimensional maps as models for representation of the dynamics. These situations may arise in the context of multi-parameter analysis of transition to chaos in multidimensional systems.

Generalizing concept of “scenario” for a multi-parameter case, we may think of some configuration of domains of distinct regimes in the parameter space, which includes regions of regular and chaotic dynamics. Generic one-parameter transitions give rise to onset of chaos at some surfaces. In particular, the Feigenbaum scenario occurs if a road in the parameter space crosses transversally a sequence of the period-doubling

bifurcation surfaces accumulating to the limit critical surface. Behaviors that are more special may occur at some curves and points on this surface. In the multi-parameter analysis, we are obliged to consider them too, as phenomena of codimensions two and three, respectively. As believed, these critical situations, like the Feigenbaum one, allow RG analysis, which must reveal the intrinsic quantitative regularities. It implies existence of universal constants responsible for scaling properties in the phase space and in the parameter space near the criticality, as attributes of the universality class. In addition, configuration of regions of different dynamical regimes in the parameter space in a definite coordinate system must be universal too. The Feigenbaum critical behavior appears in this scheme as a phenomenon of codimension one.

Critical situations of higher codimensions deserve accurate study and classification because they represent “organizing centers” of the parameter space structure, where domains of all relevant characteristic dynamical regimes of the system are concentrated locally. It is clear that practical observation of the high-codimensional critical situations is more difficult than that for the low-codimensional ones (the same is true for the high codimension bifurcations and catastrophes<sup>(25–28)</sup>). For this reason theoretical understanding of the high-codimensional types of critical behavior is of particular significance for design of experiments aimed at their realization and investigation. An important task of the theory is also construction of model systems, the simplest representatives of the universality classes, which would play for them the same role as the one-dimensional quadratic map for the Feigenbaum scenario.

The paper is organized as follows. In Section 2, we derive a two-dimensional generalization of the Feigenbaum–Cvitanović equation and explain general content of the renormalization group analysis in application to the situations of period doubling multiparameter criticality. In Section 3, we review several critical situations associated with solutions of this equation: period-doubling universality in area-preserving maps (H-type), bicritical point, which appears in a special case of two-dimensional map decomposed onto two subsystem with unidirectional coupling, and types of criticality intrinsic to non-invertible two-dimensional maps designated as FQ-type and C-type. Section 4 is devoted to discussion of the problem of observation of the mentioned types of criticality in realistic systems. In particular, we consider a model of van der Pol oscillator driven by pulses with nonlinear dependence of the amplitude on the instantaneous state. It demonstrates H-type of criticality although does not relate to conservative class. Then, we review several examples of the bicritical behavior: unidirectionally coupled Hénon maps, coupled driven dissipative oscillators, coupled chaotic self-oscillators (Chua’s circuits). A possibility of occurrence

of FQ criticality is discussed; as examples, we consider systems of mutually coupled non-identical Hénon maps and Chua's circuits. Finally, two examples of the critical behavior of C type are presented for a periodically driven chaotic oscillator of Rössler and for a model map demonstrating the Neimark–Sacker bifurcation. In conclusion, we resume the presented material and discuss it in a frame of the general picture of multi-parameter criticality in nonlinear dynamics.

## 2. GENERAL CONTENT OF THE RENORMALIZATION GROUP ANALYSIS

To analyze types of critical behavior intrinsic to two-dimensional maps due to presence of an additional dimension of phase space, we need a two-dimensional generalization of the renormalization equation of Feigenbaum–Cvitanović.<sup>(29–31)</sup> It may be derived easily under assumption that a coordinate system in the two-dimensional phase space is selected in such way that the rescaling transformation, performed in a course of the procedure, is diagonal:  $X \rightarrow X/\alpha$ ,  $Y \rightarrow Y/\beta$ .

Let us assume that evolution operator of the dynamics under consideration over  $2^k$  units of discrete time is defined by a pair of functions  $\{g_k(X, Y), f_k(X, Y)\}$  normalized in such way that  $g(0, 0) = 1$ ,  $f(0, 0) = 1$ . By two-fold application of this operator and after variable change  $X \rightarrow X/\alpha_k$ ,  $Y \rightarrow Y/\beta_k$ , where  $\alpha_k = 1/g_k(1, 1)$  and  $\beta_k = 1/f_k(1, 1)$ , we get the renormalized evolution operator for  $2^{k+1}$  units of time:

$$\begin{aligned} g_{k+1}(X, Y) &= \alpha_k g_k(g_k(X/\alpha_k, Y/\beta_k), f_k(X/\alpha_k, Y/\beta_k)), \\ f_{k+1}(X, Y) &= \beta_k f_k(g_k(X/\alpha_k, Y/\beta_k), f_k(X/\alpha_k, Y/\beta_k)). \end{aligned} \quad (1)$$

One can apply this doubling procedure called the RG transformation repeatedly to obtain a sequence of the evolution operators for larger and larger time scales. A critical situation usually corresponds to convergence of the operator sequence to some definite limit, a *fixed point of the RG transformation*, or, as alternative, to a *periodic point* called also a *cycle*. However, the last possibility is not conceptually different, because in the case of period  $p$  one can speak of a fixed point of the RG transformation composed of  $p$  steps of the original construction.

Presence of a fixed point of the RG transformation means that the rescaled long-time evolution operators at the criticality will be of a universal form, up to a characteristic scale. In principle, this form of the renormalized operator may be recovered (say, numerically) directly from the functional fixed-point equations determined entirely by structure of the RG scheme,

i.e., without any reference to a concrete system under examination. Therefore, a fixed-point solution of RG equation gives rise to a universality class. It may include systems of very different mathematical nature (e.g. iterative maps, ordinary differential equations, extended systems, etc.)

In a case of a fixed point of the doubling transformation, the equations take a form

$$\begin{aligned} g(X, Y) &= \alpha g(g(X/\alpha, Y/\beta), f(X/\alpha, Y/\beta)), \\ f(X, Y) &= \beta f(g(X/\alpha, Y/\beta), f(X/\alpha, Y/\beta)), \end{aligned} \tag{2}$$

where  $\alpha = 1/g(1, 1)$  and  $\beta = 1/f(1, 1)$ . (Some versions of these equations in different contexts were suggested and discussed e.g. in refs. 29, 32, 33.) It is worth noting that often the “scaling variables”  $X, Y$  do not coincide with “natural” variables of model maps.

The next step in the RG analysis consists in consideration of small perturbations of the solution associated with the critical situation under study. It gives rise to eigenvalue problem for a set of functional equations obtained from linearization of the RG transformation (1) near a fixed point or a periodic solution. In a case of a fixed point of doubling transformation  $\{g(X, Y), f(X, Y)\}$  the eigenvalue problem reads

$$\begin{aligned} vu(X, Y) &= \alpha [g'_1(g(X/\alpha, Y/\beta), f(X/\alpha, Y/\beta))u(X/\alpha, Y/\beta) \\ &\quad + g'_2(g(X/\alpha, Y/\beta), f(X/\alpha, Y/\beta))v(X/\alpha, Y/\beta) \\ &\quad + u(g(X/\alpha, Y/\beta), f(X/\alpha, Y/\beta))], \\ vv(X, Y) &= \beta [f'_1(g(X/\alpha, Y/\beta), f(X/\alpha, Y/\beta))u(X/\alpha, Y/\beta) \\ &\quad + f'_2(g(X/\alpha, Y/\beta), f(X/\alpha, Y/\beta))v(X/\alpha, Y/\beta) \\ &\quad + v(g(X/\alpha, Y/\beta), f(X/\alpha, Y/\beta))], \end{aligned} \tag{3}$$

where indices 1 and 2 designate derivatives in respect to the first and the second arguments.<sup>3</sup>

Among the eigenmodes one has to select the relevant ones, with  $|\nu| > 1$  (they are responsible for asymptotic behavior of the solution at subsequent repetition of the RG transformation), and exclude modes associated with infinitesimal variable changes. The number of relevant modes  $n$  corresponds to codimension of the critical situation. It is called also a degree of structural stability. This is a minimal number of control parameters needed to observe

<sup>3</sup>The form of the linearized operator may be understood by analogy with the eigenvalue problem from Feigenbaum’s theory that gives rise to the universal constant  $\delta = 4.6692\dots$ . The equations (3) appear from a straightforward generalization of the eigenvalue problem<sup>(1,2)</sup> for the two-dimensional case.<sup>(29–31, 34–36)</sup>

this criticality in a family of maps as a generic phenomenon. Indeed, as we require the coefficients at  $n$  relevant eigenvectors to vanish, we obtain precisely  $n$  conditions on parameters of the map under study.

To reveal scaling properties of the parameter space near a critical situation one has to define a special local coordinate system, “scaling coordinates”. It is natural to take the critical point itself as origin. Coordinate axes must be directed in such way that a shift in the parameter space from the critical point along each axis to give rise to a perturbation associated with one definite relevant eigenmode of the linearized RG equation. The eigenvalues  $\nu = \delta_1, \dots, \delta_n$  then play a role of scaling factors: under magnification with these factors along the coordinate axes one will observe repetition of the parameter space arrangement in smaller and smaller vicinities of the critical point. Moreover, in scaling coordinates, the  $n$ -dimensional parameter space will have a universal topography, specific for the given type of criticality. In a case of period- $p$  fixed point of the RG equation, each new level of the self-similar structure in the parameter space will correspond to  $2^p$ -tupling of the time scale.

For codimensions higher than one, the problem of explicit construction of the scaling coordinates is usually nontrivial. Let us suppose we have a critical point of codimension 2 with relevant eigenvalues  $\delta_1$  and  $\delta_2$ . One coordinate axis associated with the larger eigenvalue  $\delta_1$  may be directed almost arbitrarily. The only condition is that a shift along this direction has to contribute into the coefficient at the eigenvector associated with the largest eigenvalue. In other words, it has to be transversal to the curve, at which this coefficient vanishes. In contrast, the second coordinate axis must be defined accurately to coincide with that curve or, at least, to have a tangency of certain order with it.

In practice, expressions for parameters via scaling coordinates  $(C_1, C_2)$  may be constructed as power expansions. Moreover, it is reasonable to truncate the expansions up to a finite number of terms. Which terms must be retained, depends on a concrete relation between the eigenvalues  $\delta_1$  and  $\delta_2$ . Let us assume that  $|\delta_1| > |\delta_2|^k > 1$  at  $k = 1, \dots, K$ , but  $|\delta_2|^{K+1} > |\delta_1|$ . Then, the expressions for deflections of two control parameters from the critical point via  $C_1$  and  $C_2$  should contain the terms  $C_1, C_2, C_2^2, \dots, C_2^K$ . To explain this assertion, let us suppose that we draw a sequence of pictures for parameter plane, representing topography of vicinities of the critical point in scaling coordinates with increasing resolution: the depicted scales for the coordinate axes vary as  $C_1 \propto \delta_1^{-k}$  and  $C_2 \propto \delta_2^{-k}$ . If we review the  $k$ -th picture, due to the rescaling, the contribution of the term  $C_2^m$  in the scaling coordinate expression will be of order  $\delta_2^{-mk}$ . Neglecting this term, we would have an error of order  $\delta_2^{-mk} \delta_1^k$  in the amplitude of the

main mode growing as  $\delta_1^k$ . This error grows in dependence of the picture number  $k$ , if  $m \leq K$ , and decreases, if  $m > K$ . Taking into account for terms with  $m \leq K$  is necessary, but those with  $m > K$  may be omitted. In the case  $K = 1$ , i.e. at  $\delta_2^2 > |\delta_1|$ , the situation is the simplest: it is sufficient to use linear variable change to get the scaling coordinates.

In the case of codimension 3, one should account terms like  $C_2^k C_3^r$  with all possible integer  $r$  and  $k$ , for which  $\delta_2^k \delta_3^r < \delta_1$ .

### 3. CRITICALITY TYPES INTRINSIC TO TWO-DIMENSIONAL MAPS

#### 3.1. Period-Doubling Criticality in Area-Preserving Maps

Soon after the works of Feigenbaum, several authors paid attention to the fact that an infinite sequence of period-doubling bifurcations occurs not only in dissipative but also in conservative systems, in particular, in two-dimensional area-preserving maps.<sup>(33,34)</sup> In contrast to the dissipative case, the convergence rate is a distinct universal factor,  $\delta \approx 8.72$ . An appropriate version of the RG analysis was developed e.g. in refs. 29, 32, 34. This kind of period-doubling is often referred to as Feigenbaum’s universality for conservative systems. However, in a spirit of our approach, we prefer to separate terminologically this type of critical behavior from the classic Feigenbaum universality class. Therefore, we call it *the Hamiltonian period-doubling criticality* and designate with symbol H.

Hénon map

$$x_{n+1} = 1 - ax_n^2 - by_n, \quad y_{n+1} = x_n, \tag{4}$$

delivers a commonly known example of the H-type critical behavior at  $b = 1$ , where it becomes area-preserving and has unit Jacobi determinant.<sup>4</sup> The period-doubling bifurcation curves on the parameter plane  $(a, b)$  under increase of  $b$  approach the bifurcation points of the conservative system at  $b = 1$ . (There both Floquet multipliers of the respective periodic orbits become equal to  $-1$ .) These points form a sequence converging to the H-point located at

$$b_c = 1, \quad a_c = 4.136166803904275414860286\dots \tag{5}$$

<sup>4</sup>Note difference with original Hénon’s notation:  $b$  is changed to  $-b$ . We prefer this form because  $b > 0$  corresponds now to positive Jacobian, the case that allows physical interpretations of the Hénon map as Poincaré map e.g. for kicked rotator and kicked oscillator, see ref. 36.

This critical point is associated with a fixed-point solution of the RG equation (1) in a class of functional pairs with unit Jacobian determinant. In literature, one can find several representations of this solution,<sup>(29,31,32,34,35)</sup> in particular, in a form of expansions over powers of two variables:<sup>5</sup>

$$\begin{aligned} g(X, Y) &= 1 - 0.1947X - 0.1252Y - 0.9148X^2 - 0.0050XY + 0.0004Y^2 + \dots, \\ f(X, Y) &= 1 + 4.7901X - 2.0556Y - 14.8638X^2 + 0.1198Y^2 + 0.3204XY + \dots \end{aligned} \quad (6)$$

Renormalization constants found numerically are  $\alpha = -4.0180767046$  and  $\beta = 16.3638968792$ . Expressions for variables  $X, Y$  in the RG equation via “natural” variables of the map (4) look like  $X = x - x_c, Y = y - (1 - a_c x^2)/2$ , where  $x_c = 0.047528242662189948 \dots$

Because of conservative nature of the dynamics, there is no attractor at the critical point. Nevertheless, the phase space possesses self-similar structure. In particular, at the critical point H there exists a complete set of unstable period- $2^k$  orbits. Locally, near the origin in  $(X, Y)$ -coordinates, their elements obey the scaling property  $X \cong 1/\alpha^k, Y \cong 1/\beta^k$ . Asymptotically in  $k$ , Floquet multipliers of these orbits tend to the universal constants  $\mu_1 = -2.057478352$  and  $\mu_2 = 1/\mu_1 = -0.486031845$ . (These numbers are eigenvalues of the Jacobian matrix for the mapping  $(X, Y) \mapsto (g(X, Y), f(X, Y))$  at its fixed point.)

Numerical solution of the eigenvalue problem for the RG equation linearized near the fixed-point reveals two relevant eigenvalues,  $\delta_1 = 8.721097206$  and  $\delta_2 = 2$ .<sup>(29,31–35,37,38)</sup> The first one is associated with perturbations inside the area-preserving class, and the second responds for dissipation. As follows, for conservative systems the H criticality is a phenomenon of codimension one, and in a class of general systems it is of codimension two. Scaling coordinates in the parameter plane of the Hénon map are determined by expressions  $a - a_c = C_1 + a_c C_2 + 1.560093C_2^2, b = 1 + C_2$ , as found by combination of computations and analytical considerations.

### 3.2. Bicritical Point in a Model with Unidirectional Coupling

Let us turn now to a special class of two-dimensional non-invertible maps, which allow decomposition onto subsystems with unidirectional

<sup>5</sup>For this and other discussed types of criticality we give here shortened versions of expansions for the universal functions, only to show their structure. For more accurate data, appropriate for computations, we address a reader e.g. to our previous paper and web site, see ref. 31.



coupling:  $x_{n+1} = G(x_n)$ ,  $y_{n+1} = F(x_n, y_n)$ .<sup>(39,40)</sup> In literature, such systems were discussed, in particular, as models of turbulence in open flows.<sup>(41,42)</sup> Systems with unidirectional coupling may be constructed artificially; for example, in electronics and optics such coupling may be designed easily in experiments.<sup>(39,43)</sup> Recently, systems of this kind are studied in the context of problems of chaotic communication.<sup>(44,45)</sup>

A model example is a system of two elements, each governed by a quadratic map:<sup>(40)</sup>

$$x_{n+1} = 1 - \lambda x_n^2, \quad y_{n+1} = 1 - Ay_n^2 - Bx_n^2, \quad (7)$$

where  $\lambda$  and  $A$  are control parameters for the first (“master”) and the second (“slave”) subsystems, and  $B$  is the coupling parameter.

Figure 1 shows a chart of the parameter plane  $(\lambda, A)$  for the model (7) at fixed  $B = 0.375$ . Gray tones designate domains of regimes of different periods in the driven subsystem. At small values of  $A$  any periodic regime in the first subsystem induces the same period in the second one, so, the vertical borders in the diagram correspond to bifurcations in the first subsystem. In accordance with Feigenbaum’s law, they accumulate to the border of the onset of chaos, also depicted by a vertical line. On the other hand, going on the parameter plane bottom-up in a domain of

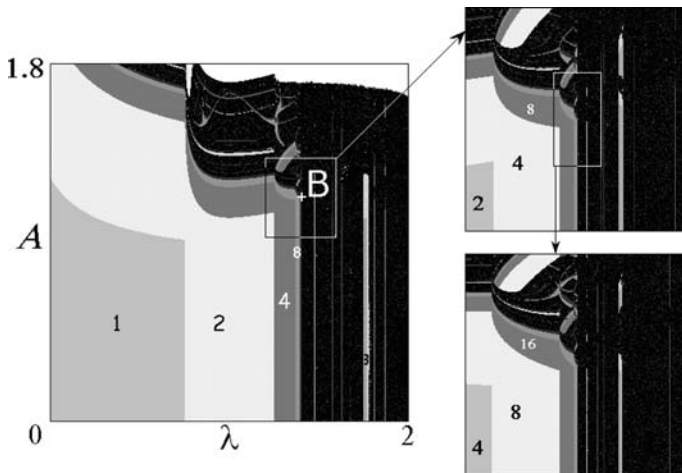


Fig. 1. Chart of dynamical regimes on parameter plane of the model map (7) at fixed coupling parameter  $B = 0.375$ . Insets show local topography in a vicinity of the bicritical point and illustrate scaling property: the picture reproduces itself under scale change by factors  $\delta_1 = 4.6692$  and  $\delta_2 = 2.3927$  along the axes  $\lambda$  and  $A$ , respectively.

period  $p=1, 2, 4, \dots$  of the first subsystem, one observes period doubling bifurcation cascade in the second subsystem, starting from period  $p$ , and then transition to chaos. The bifurcation lines are some curves, each of which has a fissure at the intersection with a bifurcation line of the first subsystem. The sequence of these curves converges to a critical line, which is a chaos border in the second subsystem.

The point at which both the critical lines meet, is called *the bicritical point*.<sup>(39,40)</sup> In the model (7) at  $B=0.375$  it is located at

$$\lambda_c = 1.401155189092\dots, \quad A_c = 1.124981403\dots \tag{8}$$

and marked with symbol B in Fig. 1.

Critical dynamics at the bicritical point is associated with a fixed-point solution of the two-dimensional RG Eq. (2) represented by a pair of functions  $\{g(x), f(x, y)\}$ , accounting the unidirectional nature of coupling. As follows from (2), they obey a set of functional equations

$$g(x) = \alpha g(g(x/\alpha)), \quad f(x, y) = \beta f(g(x/\alpha), f(x/\alpha, y/\beta)). \tag{9}$$

The first equation is independent of the second one, and  $g(x)$  is the well-known universal function of Feigenbaum and Cvitanović, with  $\alpha = 1/g(1) = -2.5029\dots$

From numerical solution of the second equation<sup>(40,31)</sup> the second component of the functional pair was obtained, as an expansion over powers of  $x^2$  and  $y^2$ :

$$f(x, y) = 1 - 0.5969x^2 - 0.0321x^4 - 0.8556y^2 - 0.3029x^2y^2 - 0.4317y^4 + \dots \tag{10}$$

The rescaling factor was also computed; it is a new universal constant  $\beta = -1.505318159\dots$

Next, we can consider perturbations of the RG equation solution due to a parameter shift from the bicritical point. Under an assumption that the perturbations do not violate the unidirectional nature of coupling, we can decompose the problem: one subspace corresponds to a class of perturbations of the first subsystem, and another to perturbations of the second one. For the first class, the problem reduces to that of Feigenbaum, and there is a unique relevant eigenmode with the eigenvalue  $\delta_1 = 4.6692\dots$  For the second class we come to equation

$$v v(x, y) = \beta [f'(g(x/\alpha), f(x/\alpha, y/\beta))v(x/\alpha, y/\beta) + v(g(x/\alpha), f(x/\alpha, y/\beta))], \tag{11}$$

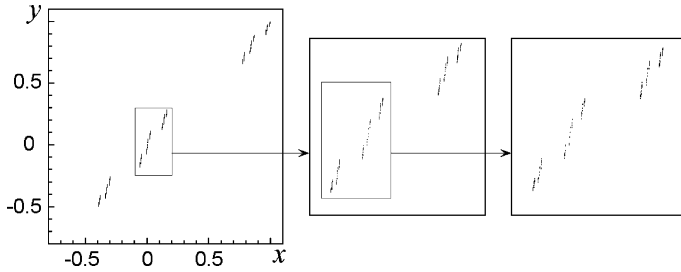


Fig. 2. Bicritical attractor and illustration of its scaling property. The insets show a vicinity of the origin with rescaling by factors  $\alpha = -2.5029$  and  $\beta = -1.5053$  along horizontal and vertical axes, respectively.

where a prime designates a derivative in respect to the second argument. Numerical solution yields the second eigenvalue  $\delta_2 = 2.3927244\dots$ . Presence of two relevant eigenvalues means that the bicritical situation has codimension 2 in a class of systems with unidirectional coupling.<sup>6</sup>

The map  $(x, y) \rightarrow \{g(x), f(x, y)\}$ , which represents asymptotic form of the evolution operator at the bicritical point, has a fixed point  $(x^*, y^*)$ , as checked numerically. Then, as follows from the RG equation, it has orbits of all periods  $2^k$ , starting at  $(x^*/\alpha^k, y^*/\beta^k)$ . All of them are unstable, and the Floquet multipliers are determined by the universal numbers  $\mu_1 = g'(x^*) = -1.6011913$  and  $\mu_2 = f'_y(x^*, y^*) = -1.17885538$ .

Attractor at the bicritical point is represented by a fractal set on the plane  $(x, y)$ , see Fig. 2. The constants  $\alpha$  and  $\beta$  determine scaling properties of this set locally near the origin  $(0, 0)$  along the axes  $x$  and  $y$ , respectively. Hausdorff dimension of the bicritical attractor was computed in ref. 40; the improved estimate yields  $D_0 = 1.0785514$ .

On the parameter plane, a neighborhood of the bicritical point obeys a scaling property. Namely, the local topography of the dynamical regimes reproduces itself in smaller scales under magnification along the axes  $\lambda$  and  $A$  with factors  $\delta_1$  and  $\delta_2$ , respectively. It corresponds to doubling of the characteristic time scales. In Fig. 1 this property is illustrated by insets.

Bicritical points with the same quantitative regularities take place in the model map (7) also at other values of the coupling parameter. In fact, in the three-dimensional parameter space there is a curve of the bicritical

<sup>6</sup>In the case of smooth perturbations including those introducing backward coupling, in accordance with our computations, spectrum of the linearized RG Eq. (3) near the fixed point solution responsible for the bicriticality contains seven relevant eigenvalues:  $\delta_1 = 4.6692016$ ,  $\delta_2 = 2.3927244$ ,  $\delta_3 = 4.296897$ ,  $\delta_4 = -4.161610$ ,  $\delta_5 = -1.83648$ ,  $\delta_{6,7} = 0.9404 \pm 0.4024i$ . Hence, codimension is rather high, and it seems very problematic to observe this type of criticality without constraint of the unidirectional coupling.

points. It is placed in interval of  $B$  from 0 to 0.83505, and the edges are critical points of distinct nature (see details in ref. 46).

In fact, bicriticality evidently may occur under much more general circumstances than that of the quadratic coupling. For example, let us turn to a model with linear coupling term:

$$X_{n+1} = 1 - \lambda X_n^2, \quad Y_{n+1} = 1 - aY_n^2 + bX_n. \quad (12)$$

By a shift of a reference point for the discrete time in the first subsystem, i.e. setting  $X_n = x_{n+1}$ , we get the map

$$x_{n+1} = 1 - \lambda x_n^2, \quad Y_{n+1} = 1 - aY_n^2 + bx_{n+1} = 1 - aY_n^2 + b(1 - \lambda x_n^2), \quad (13)$$

which transforms easily to the model (7) by means of a variable change  $Y = y(1 + b)$ ,  $B = b(1 + b)\lambda$ . Hence, the model (12) also manifests bicriticality for appropriately chosen values of the parameters.

### 3.3. Criticality of FQ-type

Let us consider a two-dimensional non-invertible map of the following special form:<sup>(47,31)</sup>

$$x_{n+1} = 1 - ax_n^2 + d \cdot x_n y_n, \quad y_{n+1} = 1 - bx_n y_n \quad (14)$$

Figure 3 shows a chart of regimes for this map on a parameter plane  $(a, b)$  at fixed  $d = 0.3$ . Gray tones designate domains of different periods. Black corresponds to non-periodic regimes, including quasiperiodicity and chaos, and white to divergence of iterations to infinity.

Obviously, at  $b = 0$  we have a quadratic map, which demonstrates a standard period-doubling cascade under increase of  $a$ . Due to the Feigenbaum universality, the same character of the transition to chaos takes place at nonzero moderate values of  $b$ . At larger  $b$  the character of dynamics changes: domains of quasiperiodicity appear alternating with domains of periodic behavior (the Arnold tongues).

Under increase of  $b$  along the Feigenbaum critical curve, we arrive at the critical point designated FQ (that stands for “Feigenbaum + Quasiperiodicity”).<sup>(47,31)</sup> To localize it accurately, one can trace a sequence of terminal points of the period-doubling bifurcation curves, where two Floquet multipliers of the respective periodic orbits becomes both equal to  $(-1)$ ,

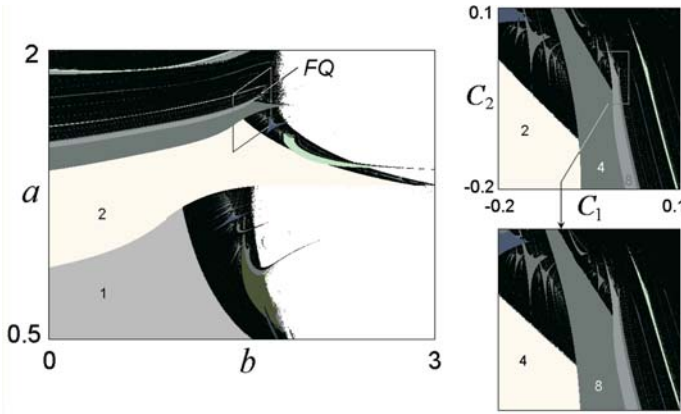


Fig. 3. Chart of dynamical regimes for the model map (14) on the parameter plane  $(a, b)$  at fixed  $d=0.3$ . A neighborhood of the critical point FQ is shown separately in the insets in scaling coordinates  $a - a_c = C_1 + 0.47733C_2$ ,  $b - b_c = C_2$ . The pictures demonstrate self-similarity under scale change with factors  $\delta_1 = 6.3263$  and  $\delta_2 = 3.4447$  along the horizontal and vertical axes, respectively.

and estimate limit of this sequence. At the selected value  $d=0.3$  the critical point FQ is placed at

$$a_c = 1.767192895 \dots, \quad b_c = 1.629678013 \dots \tag{15}$$

As found,<sup>(47,31)</sup> this critical point is associated with a fixed point of the RG Eq. (1); functions  $g$  and  $f$  are represented by expansions over powers of  $X^2$  and  $XY$ :

$$\begin{aligned} g(X, Y) &= 1 - 1.0979X^2 + 0.1571X^4 + 0.0018X^2Y^2 \\ &\quad - 0.7114XY + 0.0865X^3Y + \dots, \\ f(X, Y) &= 1 + 0.0680X^2 + 1.5416X^4 + 0.2101X^2Y^2 \\ &\quad - 2.7960XY + 1.3619X^3Y + \dots \end{aligned} \tag{16}$$

The scaling constants are  $\alpha = -1.90007167$  and  $\beta = -4.00815785$ . (A link of  $X$  and  $Y$  with the original  $x$  and  $y$  in the model (14) is expressed as  $X \propto x$ ,  $Y \propto y - 2.1091x$ .)

At the critical point FQ there exist a complete set of periodic orbits of periods  $2^k$ . Indeed, as checked numerically, the map  $(X, Y) \rightarrow \{g(X, Y), f(X, Y)\}$ , has a fixed point  $(X^*, Y^*)$ . Then, as follows from the RG equation, it has an orbit of period  $2^k$ , starting at  $(X^*/\alpha^k, Y^*/\beta^k)$  for

any integer  $k$ . All these orbits are unstable, with Floquet multipliers determined by eigenvalues of the matrix  $\begin{pmatrix} g'_X(X^*, Y^*) & g'_Y(X^*, Y^*) \\ f'_X(X^*, Y^*) & f'_Y(X^*, Y^*) \end{pmatrix}$ . These are universal numbers  $\mu_1 = -1.579739$  and  $\mu_2 = -1.057149$ .

Attractor at the critical point FQ is a fractal set, which may be thought as a limit object, “cycle of period  $2^\infty$ ”. The first diagram of Fig. 4 shows a general view of the critical attractor on the phase plane  $(x, y)$  of the model map (14) at  $d = 0.3$ . The second and the third diagrams are plotted in coordinates used in the RG equation. In these coordinates, the structure reproduces itself under magnification with factors  $\alpha$  and  $\beta$  along the horizontal and vertical axes, respectively.

Numerical solution of the eigenvalue problem for the RG equation linearized at the fixed point FQ yields three relevant eigenvalues,  $\delta_1 = 6.32631925$ ,  $\delta_2 = 3.44470967$ , and  $\delta_3 = \alpha = -1.90007167$ .<sup>(31)</sup> Hence, formally speaking, the codimension is three. Nevertheless, due to special selection of the model map (14), shifts of the parameters from the critical point do not contribute into the third mode. This is why we could detect the critical point FQ in a course of two-parameter analysis. In the parameter space  $(a, b, d)$  there is a curve of FQ points. The scaling property for a cross-section of the parameter space by a surface transversal to the critical curve is determined in this situation by two factors,  $\delta_1$  and  $\delta_2$ . It is illustrated by insets in Fig. 3. An expression for the scaling coordinates is given in the figure capture.

A model, for which variation of parameters gives rise to all three relevant modes of the linearized RG equation, may be constructed by adding one more parameter:

$$x_{n+1} = 1 - ax_n^2 + d(x_n - c)y_n, \quad y_{n+1} = 1 - b(x_n - c)y_n. \quad (17)$$

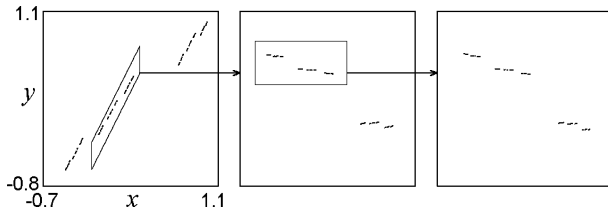


Fig. 4. Critical attractor at the point FQ in the model map (14) at  $d = 0.3$  and illustration of its scaling property. A selected fragment (parallelogram) is shown separately in “scaling coordinates”  $X = x$ ,  $Y = y - 2.1091x$ . Under magnification by factors  $\alpha = -1.9000$  and  $\beta = -4.0081$  along the horizontal and vertical axes, respectively, the structure reproduces itself with good accuracy.

This model delivers the three-parameter unfolding of the FQ critical point. (See ref. 47, where charts of regimes are shown in different cross-sections of the parameter space for the model (17).)

**3.4. Criticality of C-type**

All types of critical situations discussed so far relate to some special classes of two-dimensional maps (H to an area-preserving class, B to a class allowing the master-slave decomposition, FQ to a case of certain degeneracy). Of what kind may be critical behavior in a generic non-invertible two-dimensional map?

As proved by Whitney,<sup>(26,48)</sup> two types of singularities may occur as typical in two-dimensional differentiable maps, a fold and a cusp. In two-dimensional state space, the folds take place on curves and cusps at single points.

To derive a convenient model of iterative map, let us start with a standard form of the fold mapping

$$(u, v) \mapsto (u^2, v) \tag{18}$$

and compose it with a general affine transformation  $(u, v) \mapsto (A + Bu + Cv, D + Eu + Fv)$ , where  $A, B, \dots, F$  are parameters. It yields a map

$$(u, v) \mapsto (A + Bu^2 + Cv, D + Eu^2 + Fv), \tag{19}$$

which may be reduced by a variable and parameter change

$$\begin{aligned} x &= -Bu, & y &= [D/(1 - F) - v]B^2F^{-1}, \\ a &= B[CD/(F - 1) - A], & b &= EC/B, & d &= F \end{aligned} \tag{20}$$

to the three-parameter map<sup>(47)</sup>:

$$x_{n+1} = a - x_n^2 + by_n, \quad y_{n+1} = -x_n^2 + d \cdot y_n. \tag{21}$$

Figure 5 shows a chart of dynamical regimes on the parameter plane  $(a, d)$  at fixed  $b = -0.6663$  (a reason for this special choice is explained further). At small  $d$ , as seen from the picture, increase of  $a$  is accompanied by transition to chaos via period doubling cascade, and it obeys, as checked, the Feigenbaum regularities. Increasing  $d$  and tracing one of the

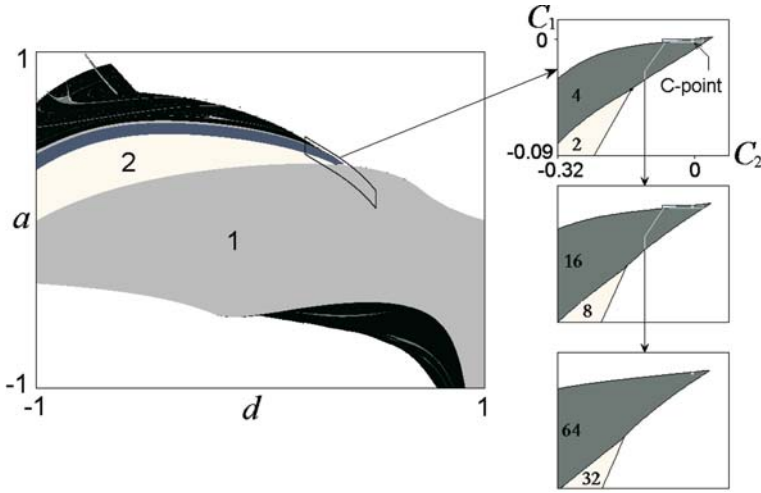


Fig. 5. Chart of dynamical regimes for the model map (21) at  $b = -0.6663$  (left) and areas of stability for cycles of period 2, 4, ..., 64 in scaling coordinates  $a - a_c = C_1 - C_2 - 1.54607C_2^2 - 2.15C_2^3$ ,  $d - d_c = 0.79017C_2$  (to the right).

period-doubling bifurcation curves, we arrive at the terminal point, where two Floquet multipliers of the periodic orbit become equal to  $(-1)$  and  $1$ . Accurate estimate of the limit of the sequence of terminal points from numerical computations yields coordinates of the critical point

$$a_c = 0.24990280\dots, \quad d_c = 0.45290288\dots \tag{22}$$

Computations based on iterations of the model map at this point with use of “scaling variables”  $X = x$ ,  $Y = y + 1.3164475$  show that the respective solution of the RG Eq. (1) is represented by a period-2 cycle. It consists of two functional pairs  $(g_1(x, y), f_1(x, y))$  and  $(g_2(x, y), f_2(x, y))$ , which satisfy a set of functional equations

$$\begin{aligned} g_2(X, Y) &= \alpha_1 g_1(g_1(X/\alpha_1, Y/\beta_1), f_1(X/\alpha_1, Y/\beta_1)), \\ f_2(X, Y) &= \beta_1 f_1(g_1(X/\alpha_1, Y/\beta_1), f_1(X/\alpha_1, Y/\beta_1)), \\ g_1(X, Y) &= \alpha_2 g_2(g_2(X/\alpha_2, Y/\beta_2), f_2(X/\alpha_2, Y/\beta_2)), \\ f_1(X, Y) &= \beta_2 f_2(g_2(X/\alpha_2, Y/\beta_2), f_2(X/\alpha_2, Y/\beta_2)). \end{aligned} \tag{23}$$

where  $\alpha_{1,2} = 1/g_{1,2}(1, 1)$ ,  $\beta_{1,2} = 1/f_{1,2}(1, 1)$ . (Notation “C” for this type of criticality stands for “Cycle”.) From numerical solution of these equations, the functions  $g_{1,2}$  and  $f_{1,2}$  were obtained in a form of expansions over powers of  $X^2$  and  $Y$ :



$$\begin{aligned}
 g_1(X, Y) &= 1 - 1.2770X^2 - 0.4995Y + 0.1391X^2Y + \dots, \\
 f_1(X, Y) &= 1 - 2.3210X^2 + 0.2267Y + 0.5051X^2Y + \dots, \\
 g_2(X, Y) &= 1 - 1.5293X^2 + 0.2314Y - 0.0592X^2Y + \dots, \\
 f_2(X, Y) &= 1 - 1.6598X^2 + 1.3491Y + 0.2212X^2Y + \dots
 \end{aligned}
 \tag{24}$$

As known, Feigenbaum’s RG transformation is called the doubling transformation. In our case, what we have is the *quadrupling transformation*, which possesses two fixed points represented by the functional pairs  $g_1, f_1$  and  $g_2, f_2$ . Rescaling factors determining scaling properties of the state space under this quadrupling transformation are

$$\alpha = \alpha_1\alpha_2 = 6.565350\dots, \quad \beta = \beta_1\beta_2 = 22.120227\dots, \tag{25}$$

Computations show that the map  $(x, y) \mapsto (g_1(x, y), f_1(x, y))$  possesses a *stable fixed point*  $X^* = 0.25039, Y^* = 1.59489$  with Floquet multipliers  $\mu_1^{(1)} = -0.725255$  and  $\mu_2^{(1)} = 0.847450$ , eigenvalues of the matrix  $\begin{pmatrix} g'_{1,X}(X^*, Y^*) & g'_{1,Y}(X^*, Y^*) \\ f'_{1,X}(X^*, Y^*) & f'_{1,Y}(X^*, Y^*) \end{pmatrix}$ . Recall that the map  $(x, y) \mapsto (g_1(x, y), f_1(x, y))$  iterated four times reproduces itself under scale change  $(X \rightarrow X/\alpha, Y \rightarrow Y/\beta)$ . So, *presence of the stable fixed point implies existence of stable cycles of all periods  $4^k, k = 1, 2, \dots, \infty$* , and all of them have multipliers equal to the above universal values. (Note that at least one point of a periodic orbit of period  $4^k$  from this set may be easily estimated:  $X^*/\alpha^k, Y^*/\beta^k$ .) Thus, the map  $(x, y) \mapsto (g_1(x, y), f_1(x, y))$  has an infinite countable set of coexisting attractors, the stable orbits of period  $4^k$  called *the critical quasi-attractor*.<sup>(31,47)</sup> The same is true for the model map (21) at the C-type critical point. Figure 6 shows three first representatives of this set of coexisting attractors, the orbits of period 1, 4 and 16 on the phase plane of the map (21).

Beside the stable cycles of period  $4^k$  there exist a countable set of unstable cycles of period  $2 \cdot 4^k$  at the critical point. It follows from the fact that the map  $(x, y) \mapsto (g_1(x, y), f_1(x, y))$  has a period-2 cycle with multipliers  $\mu_1^{(2)} = -0.848865$  and  $\mu_2^{(2)} = 1.174459$ . Note that the map  $(x, y) \mapsto (g_2(x, y), f_2(x, y))$  has an unstable fixed point with multipliers  $\mu_1^{(2)}, \mu_2^{(2)}$  and a stable period-2 cycle with multipliers  $\mu_1^{(1)}, \mu_2^{(1)}$ .

Linearization of Eqs. (1) gives rise to an eigenvalue problem for perturbations of the RG equation cycle. The largest three eigenvalues for the quadrupling transformation (excluding those associated with infinitesimal variable changes) are  $\delta_1 = 92.43126348, \delta_2 = 4.19244418, \delta_3 \approx 0.93$ . Only  $\delta_1$  and  $\delta_2$  are larger than 1, so, the codimension formally equals 2. It means

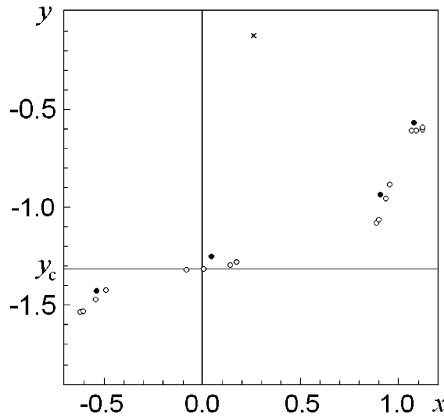


Fig. 6. Coexisting attractors of the map (21) at the critical point  $C$  for  $b = -0.6663$ : a fixed point ( $\times$ ) and stable orbits of period 4 ( $\bullet$ ) and 16 ( $\circ$ ).

that this type of critical behavior occurs as typical under two-parameter analysis. Insets in Fig. 5 illustrate the scaling property in the parameter space near the critical point  $C$  of the model map (21). In this domain, the chart of dynamical regimes may be thought as a set of overlapping sheets, each corresponding to one of the attractors coexisting at the critical point and in its vicinity. In appropriate local coordinate system (see the figure caption), the topography clearly looks self-similar under rescaling with factors  $\delta_1$  and  $\delta_2$  along the coordinate axes accompanied by quadrupling of time scales of the dynamics.

Note that the third eigenvalue  $\delta_3$  is slightly less than one. In general, it leads to very slow convergence. In other words, as a rule, the quantitative universality of  $C$  type may be observed only after a large number of period doublings. If the system has an additional third parameter, one can try to select it to remove a contribution of the slow mode. This is a reason why we choose special value of  $b = -0.6663$  for the computations. As well, the critical point  $C$  may be found at positive  $b$ . The best convergence occurs at  $b = 0.6544$ , and the critical point is located at  $a_c = 0.566620683\dots$ ,  $d_c = 1.597132592\dots$ . At this point, the RG cycle oscillates in opposite phase, and the critical quasiattractor consists of stable cycles of periods  $2 \cdot 4^k$ .

#### 4. PERIOD-DOUBLING CRITICAL BEHAVIOR IN PHYSICAL SYSTEMS AND REALISTIC MODELS

Feigenbaum's universal behavior associated with the generic period-doubling transition to chaos occurs in many nonlinear dissipative systems

of different physical nature. Equipped with knowledge of types of the period-doubling criticality intrinsic to two-dimensional maps, we may now turn to consideration of possibilities of their observation in various systems and their realistic models.

#### 4.1. H-type Criticality in the Context of Dissipative Dynamics

H-type of critical behavior was discovered as an attribute of conservative dynamics. Concerning real systems, it could occur in situations like motion of charged particles in vacuum in electric and magnetic fields, or in systems of celestial mechanics with gravitational interaction. In more common every-day circumstances, or in laboratorial studies, dissipation presents inevitably. If one wish to approach H-type criticality, say, in experiments with a forced nonlinear oscillator actualized as a mechanical device or an electronic circuit, a natural and straightforward idea is to undertake measures to exclude, as far as possible, the energy loss. In this case, in principle, we may speak only of more or less satisfactory approximation for an ideal conservative system.<sup>7</sup>

Alternatively, we may try to arrange H-type of criticality not in conservative, but in a dissipative self-oscillatory system. In this case, H type will appear not due to vanishing dissipation, but due to compensation of dissipation in the self-oscillatory system from external non-oscillatory source of energy. Accounting the codimension-2 nature of the H criticality outside the class of conservative systems, we must have two control parameters, one responsible for strength of nonlinearity, and another for the energy balance in the system.

In a more general frame, let us suppose that we have some multi-dimensional nonlinear dissipative system demonstrating the Feigenbaum period-doubling cascade, and by variation of parameters get a situation of approach of an additional mode to an instability threshold. Is it possible in such case to meet the critical behavior of H type?

As a model, let us consider a van der Pol oscillator driven by a sequence of short pulses of period  $T$ , and assume that amplitudes of the kicks depend on an instantaneous value of the dynamical variable as  $F(x)$ . Then, the dynamical equation reads

$$\ddot{x} - (\varepsilon - \mu x^2)\dot{x} + x = \sum_m F(x)\delta(t - mT), \quad (26)$$

where  $\varepsilon$  and  $\mu$  are internal parameters of the oscillator.

<sup>7</sup>In this case, in a course of the bifurcation cascade, the first period-doubling bifurcations will demonstrate (approximately) regularities intrinsic to the conservative case, and subsequent bifurcations manifest passage to the Feigenbaum law intrinsic to dissipative systems. There is a number of publications devoted to this phenomenon called *crossover*.<sup>(33,37,38,49)</sup>

Let us derive an explicit stroboscopic Poincaré map for this system in some reasonable approximation. In assumption that parameters  $\varepsilon$ ,  $\mu$ , and amplitude  $F$  are small, between the kicks we can use a method of slow amplitudes. Let us set  $x = ae^{it} + a^*e^{-it}$  and require the complex amplitudes  $a$  and  $a^*$  to satisfy an additional condition  $\dot{a}e^{it} + \dot{a}^*e^{-it} = 0$ , hence,  $\dot{x} = v = ia e^{it} - ia^* e^{-it}$ . Substitution of the expressions for  $x$  and  $\dot{x}$  into the van der Pol equation with subsequent multiplying by  $e^{-it}$  and averaging over a period of the basic oscillations yields the amplitude equation

$$\dot{a} = \frac{1}{2}\varepsilon - \frac{1}{2}\mu|a|^2 a. \quad (27)$$

Let us assume that  $x$  and  $\dot{x} = v$  are the values of coordinate and velocity just before a kick. Then, immediately after the kick, we get  $x_{+0} = x$ ,  $v_{+0} = v + F(x)$ . As follows from definition of the amplitude  $a$ ,

$$a_{+0} = a - \frac{1}{2}iF(x). \quad (28)$$

Solution of Eq. (27) with initial condition (28) yields

$$a(t) = \frac{1}{2}(x - iv) \exp(it) = \frac{a_{+0} \exp(\varepsilon t/2)}{\sqrt{1 + (\mu/\varepsilon)(\exp \varepsilon t - 1)|a_{+0}|^2}}. \quad (29)$$

At  $t = T$ , accounting the link between variables  $a$ ,  $a^*$  and  $x$ ,  $v$ , we get the coordinate and velocity just before the next kick:

$$\begin{aligned} x' &= B [x \cos T + (v + F(x)) \sin T] \{1 + C [x^2 + (v + F(x))^2]\}^{-1/2}, \\ v' &= B [-x \sin T + (v + F(x)) \cos T] \{1 + C [x^2 + (v + F(x))^2]\}^{-1/2}, \end{aligned} \quad (30)$$

where  $B = \exp \frac{1}{2}\varepsilon T$ ,  $C = \mu T (\exp \varepsilon T - 1) / (4\varepsilon T)$ . This is the desired stroboscopic map.

For simplicity, let us set  $T = (4k + 1)\pi/2$  and select a concrete function  $F(x) = 1 - Ax^2$ . Then, the map takes a form

$$\begin{aligned} x_{n+1} &= B(1 - Ax_n^2 - y_n) \{1 + C [x_n^2 + (1 - Ax_n^2 - y_n)^2]\}^{-1/2}, \\ v_{n+1} &= Bx_n \{1 + C [x_n^2 + (1 - Ax_n^2 - y_n)^2]\}^{-1/2}, \end{aligned} \quad (31)$$

where index  $n$  numerates steps of discrete time. Note that in a limit  $\varepsilon \rightarrow 0$ ,  $\mu \rightarrow 0$  we have  $B = 1$ ,  $C = 0$ , and the map (31) reduces to the area-preserving Hénon map.

Figure 7 shows a chart of dynamical regimes for the model (31) at certain fixed  $\mu T$ . The horizontal axis corresponds to parameter, which controls the Andronov – Hopf bifurcation of birth of a limit cycle in the autonomous van der Pol oscillator, and the vertical axis to parameter of nonlinearity in the kick amplitude dependence. Gray tones denote periodic behaviors with periods labeled by numbers; black corresponds to non-periodic regimes (quasiperiodicity and chaos). Strips designate areas of multistability, the alternating tones relate to the regimes associated with the distinct coexisting attractors.

At large negative  $\varepsilon$ , far from the Andronov-Hopf bifurcation threshold, the oscillator itself behaves as a linear system, and nonlinearity enters into play only due to the kick amplitude dependence on  $x$ . In this domain, the map is equivalent (up to a variable change) to the conventional Hénon map and manifests transition to chaos via the Feigenbaum period doubling cascade. In domain of positive  $\varepsilon$ , the oscillator becomes active, and a possibility of quasiperiodic behavior due to beating of its own oscillations and periodic kicks arises (see the right-hand part of the diagram).

If we increase  $\varepsilon$  and try to trace the Feigenbaum critical line, it terminates at some point. Accurately, location of this point may be estimated as a limit of the sequence of terminal points for the curves of subsequent

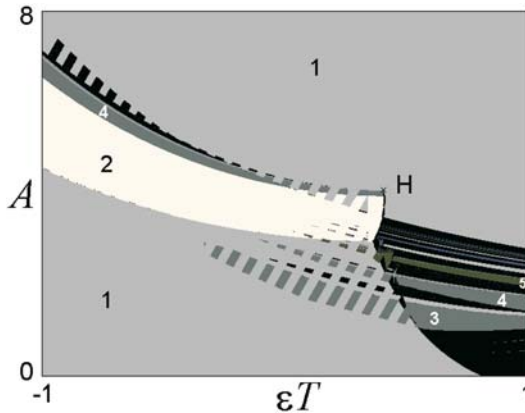


Fig. 7. Parameter plane for the map (31) at constant  $\mu T$ . Horizontal axis corresponds to the parameter controlling the Andronov – Hopf bifurcation in the autonomous van der Pol oscillator, and the vertical axis to the parameter of nonlinearity in the kick amplitude dependence. Gray tones designate periodic behaviors with periods labeled by numbers, black corresponds to chaos. Strips denote areas of multistability, the alternating tones designate regimes associated with the distinct coexisting attractors. The critical point (32) is marked with letter H. The value of  $\mu T = 3.2468323108$  has been selected numerically to have  $C = 1$  at the critical point.

period-doubling bifurcations. At those points the respective periodic orbits have two Floquet multipliers equal to  $(-1)$ . Estimating the limit, we get the critical point

$$\varepsilon T_c = 0.4036684037636\dots, \quad A_c = 4.083016502041\dots \quad (32)$$

What is nature of this point? Does it relate indeed to the H-type criticality class?

The best way to check belonging of the critical point associated with period doubling to a supposed universality class, consists in computation of multipliers for orbits of period  $2^k$  with large integer  $k$ . This is convenient, in particular, because multipliers are invariant in respect to selection of a coordinate system in the phase space. The multipliers must tend to the universal values obtained from the RG analysis for the given universality class.

For the critical point under consideration the results are summarized in Table I. Observe fast convergence to the universal constants expected for the H-type critical point in accordance with results of the RG analysis (the last row in the table). Also, as seen from the Table, a product of two multipliers for higher periods of cycles tends to 1 with high precision, which corresponds to the conservative nature of the critical dynamics in asymptotic of large time scales.

**Table I. Multipliers of cycles of period  $2^k$  and their products at the critical point of H type in the Hénon–van der Pol map (31)  $A = 4.083016502041034$ ,  $B = 1.223645113234917$ ,  $C = 1$ ,  $\varepsilon T = 0.4036684037636123$ ,  $\mu T = 3.246832310801523$**

$p = 2^k$	$\mu_1$	$\mu_2$	$\mu_1\mu_2$
1	-2.141639	-0.5135136	1.0997609
2	-2.046802	-0.4827731	0.9881407
4	-2.058910	-0.4864611	1.0015799
8	-2.057285	-0.4859759	0.9997908
16	-2.057504	-0.4860392	1.0000278
32	-2.057475	-0.4860309	0.9999963
64	-2.057477	-0.4860325	1.0000005
128	-2.057461	-0.4860359	1.0000000
256	-2.057328	-0.4860676	1.0000002
RG	-2.0574783	-0.4860318	1

### 4.2. Examples of Bicritical Behavior

The model system with bicritical point discussed in Sec.3.2 had a structure of two elements with unidirectional coupling, each governed by a one-dimensional period-doubling map. As we believe, the principal thing for the building blocks is not their one-dimensional nature, but relation to the class of the Feigenbaum period doubling systems. If so, any two systems with unidirectional coupling, in which the period doubling cascade takes place, are appropriate.

Coupling in Eq. (7) is of *dissipative type*: it tends to equalize an instantaneous state of the driven subsystem to that of the master one. Indeed, each step of iterations in that model may be regarded as a composition of a nonlinear transformation for states of uncoupled elements, and averaging of them with some weights to get the state of the driven subsystem. (See discussion for a case of mutual coupling e.g. in refs. 50, 51.) Hereafter, we often use the dissipative coupling, as its idea is clear and physically significant.

A fundamental imperfection of non-invertible one-dimensional maps consists in the fact that they cannot serve as Poincaré maps for flow systems (differential equations), at least in rigorous and straightforward sense. To make a step to more realistic models, we turn to a system of elements, each governed by a Hénon-like map. That is a two-dimensional invertible dissipative map manifesting the period-doubling cascade, and it may be regarded as Poincaré map for some flow. Using an assumption of dissipative nature of the unidirectional coupling, we set

$$\begin{aligned}
 x_{n+1} &= 1 - \lambda x_n^2 - bu_n, \\
 u_{n+1} &= x_n, \\
 y_{n+1} &= 1 - Ay_n^2 - B(\lambda x_n^2 + bu_n) - bv_n, \\
 v_{n+1} &= y_n.
 \end{aligned}
 \tag{33}$$

Here  $x$  and  $u$  relate to the master subsystem, and  $y$  and  $v$  to the driven one. Parameters  $\lambda$  and  $A$  control period-doubling, respectively, in the first and in the second subsystem.  $B$  is coupling constant, and  $b$  characterizes the dissipation strength in the subsystems. Hereafter we fix  $b=0.3$  and  $B=0.3$ .

To locate the bicritical point on the parameter plane  $(\lambda, A)$  one can trace a sequence of terminal points on the bifurcation lines  $\lambda = \lambda_k$  of period-doubling in the first subsystem, at which the second subsystem undergoes the period-doubling bifurcation too, i.e. two main multipliers of the respective periodic orbit are equal to  $-1$ . Estimate of the limit of this sequence in computation yields

$$\lambda = \lambda_c = 1.9516464506803\dots, \quad A = A_c = 1.49457524\dots \tag{34}$$

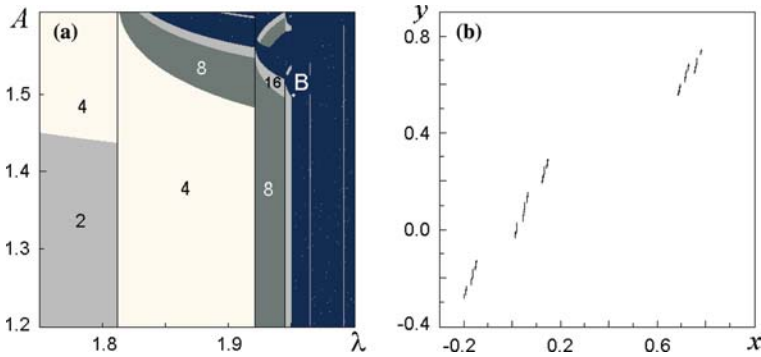


Fig. 8. Parameter plane (a) and bicornal attractor in projection onto the plane  $(x, y)$  (b) for the system of coupled Hénon maps. In diagram (a) the bicornal point is labeled with the letter B; gray tones designate areas of periodic regimes and numbers indicate periods in the driven subsystem. Dark areas correspond to chaos or unrecognized higher-period regimes. Parameter of dissipation  $b=0.3$ , and coupling parameter  $B=0.3$ .

The first subsystem obviously belongs to the Feigenbaum universality class. Hence, to check relation to the bicornal situation, it is sufficient to consider only multipliers associated with the second subsystem. In Table II we summarize the data for the critical point (34). Observe good agreement with the universal constant for higher period cycles.

Figure 8a shows a parameter plane diagram for the coupled Hénon maps, the bicornal point is marked with a letter B. Figure 8b presents a portrait of the critical attractor in projection from the four-dimensional state space onto the plane  $(x, y)$ . Both pictures look remarkably similar to those from Figs. 1 and 2. All these observations give evidence that we deal indeed with the critical point relating to the universality class discussed in Section 3.2.

**Table II. Multipliers of unstable cycles of period  $p=2^k$  in the driven subsystem for the unidirectionally coupled Hénon maps at the bicornal point  $b=B=0.3$ ,  $\lambda = \lambda_c = 1.95164645\dots$ ,  $A=A_c = 1.49457524\dots$**

$p=2^k$	$\mu$	$p=2^k$	$\mu$	$P=2^k$	$\mu$
1	-1.239263	32	-1.177933	1024	-1.177997
2	-1.280900	64	-1.176060	2048	-1.179348
4	-1.194400	128	-1.177747	4096	-1.178346
8	-1.154316	256	-1.177668	...	...
16	-1.163422	512	-1.179486	RG	-1.178855



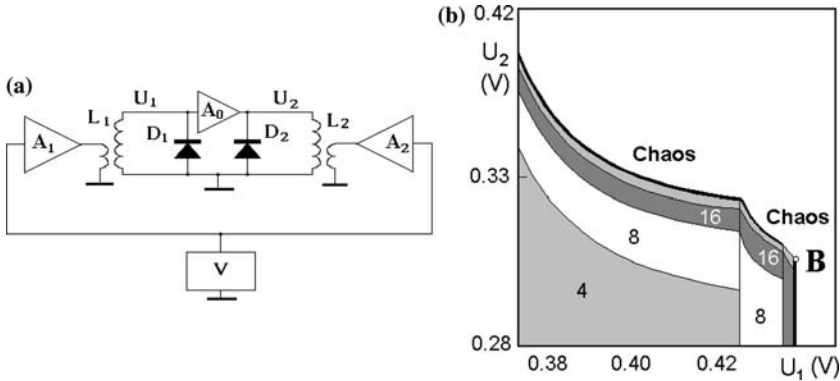


Fig. 9. Scheme of the experimental device studied in ref. 39 (a), which contains a source of alternate voltage  $V$ , amplifiers  $A_1$  and  $A_2$  with controlled gain to vary the amplitudes  $U_1$  and  $U_2$ , diodes  $D_1$  and  $D_2$ , an amplifier  $A_0$  providing the unidirectional coupling, and a chart of regimes from the experiment (b). Along horizontal and vertical axes amplitudes are plotted of driving in the first and the second subsystem, respectively.

Next, we turn to examples relating to a class of unidirectionally coupled driven dissipative nonlinear oscillators.

Already in the first work reported on the discovery of the bicritical behavior,<sup>(39)</sup> beside theoretical considerations and computations, some experimental results were presented for a system of two periodically driven nonlinear RL-diode circuits. In the scheme, the unidirectional coupling was arranged by a special amplifier (Fig. 9a). By variation of two control parameters, which were amplitudes of external driving in both subsystems, in the experiment it was sufficiently easy to bring simultaneously both subsystems to the chaos threshold and get the bicritical situation. In Fig. 9b a parameter plane chart from that experiment is reproduced. Observe nice qualitative correspondence of the topography in a vicinity of the bicritical point with that for model systems of coupled maps.

Kim and Lim<sup>(52)</sup> presented a detailed computational study for a system of driven nonlinear oscillators with unidirectional coupling:

$$\begin{aligned}
 \dot{x}_1 &= y_1, \\
 \dot{y}_1 &= -2\pi(\beta\Omega y + \Omega^2 - A \cos 2\pi t) \sin 2\pi x_1, \\
 \dot{x}_2 &= y_2 + c(x_1 - x_2), \\
 \dot{y}_2 &= -2\pi(\beta\Omega y + \Omega^2 - B \cos 2\pi t) \sin 2\pi x_2 + c(y_1 - y_2).
 \end{aligned}
 \tag{35}$$

In these equations, variables with subscripts 1 and 2 relate to the first and the second subsystem, respectively. In accordance with argumentation developed e.g. in refs. 50, 51, coupling in this system is of dissipative type

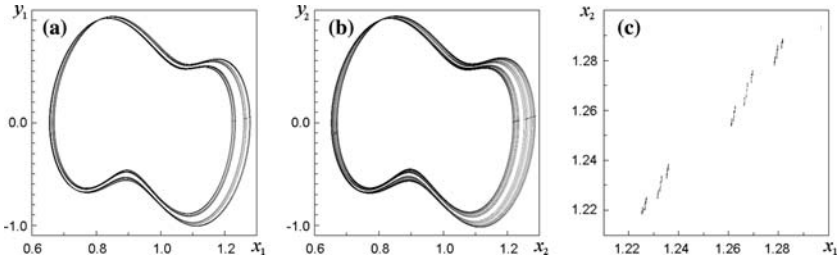


Fig. 10. Phase portraits of the bicritical attractor for the system of driven nonlinear oscillators with unidirectional coupling (35) at  $\beta = 1$ ,  $\Omega = 0.5$ ,  $c = 0.2$ ,  $A = 0.79804918$ ,  $B = 0.80237721$ . Diagrams (a) and (b) show two projections of the attractor, one onto the plane of variables of the master subsystem, and another for the driven subsystem. Black dots on the portraits correspond to the cross-section with a hyper-plane  $t = 0.35 \pmod{1}$  (stroboscopic Poincaré section). Diagram (c) represents these points on the plane of  $x_2$  versus  $x_1$ .

because it is introduced by terms in the differential equations with the same variables as those under derivatives in the left parts of the equations.

As computed in ref. 52, at fixed  $\beta = 1$ ,  $\Omega = 0.5$ , and coupling constant  $c = 0.2$ , the bicritical point of the system (35) is located at  $A = A_c = 0.79804918$ ,  $B = B_c = 0.80237721$ .

Diagrams (a) and (b) in Fig. 10 show phase portraits of the bicritical attractor in two projections from the five-dimensional extended phase space. The first is a plane of variables for the master subsystem, and another for the driven subsystem. The trajectories constituting the attractor are drawn in gray. Black dots correspond to moments of cross-section of an orbit with a hyper-plane  $t = \text{const}$  in the phase space (stroboscopic Poincaré section). Diagram (c) represents these points on the plane  $(x_1, x_2)$ . It looks remarkably similar to portraits of the bicritical attractors discussed above for the model maps. Figure 11 shows parameter plane charts locally near the bicritical point. The scaling property for a vicinity of the bicritical point is illustrated: Under magnification with factors  $\delta_1 = 4.6692$  and  $\delta_2 = 2.3927$  the structure of the domains in the parameter plane obviously looks similar.

The above examples of bicriticality relate to coupled maps and coupled non-autonomous oscillators. Is it possible to observe the phenomenon in a case of autonomous self-oscillating period-doubling systems with unidirectional coupling? Apparently, the driven subsystem must be synchronized by the master one, in a sense of phase synchronization.<sup>(53)</sup> In opposite case, for example at large frequency detuning of the elements, one should expect rather quasiperiodic dynamics with further bifurcations on a base of these regimes.

An appropriate object to construct an example of bicriticality in autonomous coupled systems is Chua's circuit, which can demonstrate

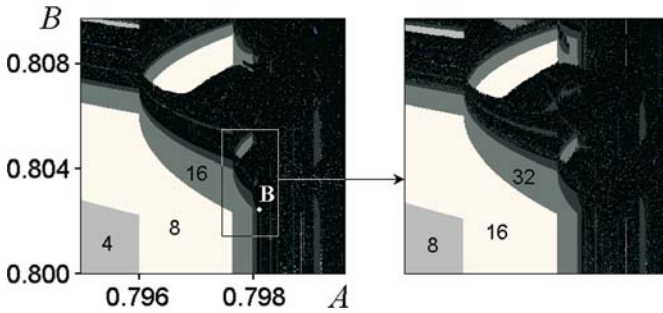


Fig. 11. Parameter plane diagrams for driven nonlinear oscillators with unidirectional coupling of Kim and Lim (35),  $\beta = 1$ ,  $\Omega = 0.5$ ,  $c = 0.2$ . Areas of distinct periodic regimes are shown in gray scale, and periods are marked with numbers. The second picture is obtained by magnification of the small box from the first one with factors  $\delta_1 = 4.6692$  and  $\delta_2 = 2.3927$  along the horizontal and vertical axes, respectively.

the Feigenbaum period-doubling cascade in a course of transition to chaos.<sup>(51,54,55)</sup> An advantage of this example is simplicity in computations: due to piecewise characteristic of the involved nonlinear element, the calculations may be performed with use of analytical expressions valid in definite parts of the phase space.

To build a model analogous to those discussed above, let us consider a system of two Chua’s circuits with unidirectional coupling of dissipative type.<sup>(51)</sup> As it tends to equalize instantaneous states of the coupled elements, it provides the phase synchronization too. The set of equations reads:

$$\begin{aligned}
 \dot{x}_1 &= \alpha_1 (y_1 - h(x_1)), & \dot{x}_2 &= \alpha_2 (y_2 - h(x_2)) + \varepsilon(x_1 - x_2), \\
 \dot{y}_1 &= x_1 + y_1 - z_1, & \dot{y}_2 &= x_2 + y_2 - z_2 + \varepsilon(y_1 - y_2), \\
 \dot{z}_1 &= -by_1, & \dot{z}_2 &= -by_2 + \varepsilon(z_1 - z_2),
 \end{aligned}
 \tag{36}$$

where

$$h(x) = \begin{cases} (2x + 3)/7, & x \leq -1, \\ -x/7, & -1 < x < 1, \\ (2x - 3)/7, & x \geq 1. \end{cases}$$

Dynamical variables  $x_i$ ,  $y_i$ ,  $z_i$  with indices  $i = 1, 2$  relate to the first and the second subsystem, respectively. Parameters  $\alpha_1$  and  $\alpha_2$  are supposed to be varied independently to control period doublings in two subsystems. Parameter  $b$  and coupling constant  $\varepsilon$  are fixed, namely, we set  $b = 10$  and  $\varepsilon = 0.2$ .

With increase of parameter  $\alpha_1$ , transition to chaos in the first subsystem occurs via the Feigenbaum period doubling bifurcation cascade and

gives rise to an asymmetric attractor of Rössler type. The limit point of the period doubling corresponds to  $\alpha_1 = 6.542725993\dots$ . At this value, by variation of parameter  $\alpha_2$ , one can reach the bicritical point at  $\alpha_2 = 6.64680875\dots$  (see details of the computations in ref. 51). For the second subsystem, as checked, multipliers at this point demonstrate fast convergence to the universal number  $-1.1788\dots$  (see Table III).

In Fig. 12 phase portraits are shown for the bicritical attractor in the coupled Chua circuits. The diagrams (a) and (b) correspond to projections of the attractor onto the planes of two variables relating to the first and to the second subsystem, respectively. Qualitatively, they may be compared with the portraits in Fig. 10. To demonstrate scaling properties intrinsic to the dynamics at the bicritical point we show separately a sequence of fragments for both pictures. Resolution of each next level of the Cantor-like structure of strips constituting the attractor requires scale change with Feigenbaum's scaling factor  $-2.5029\dots$  for the panel (a) and with bicritical factor  $-1.505318\dots$  for the panel (b).

Figure 13 shows a chart of the parameter plane  $(\alpha_1, \alpha_2)$  for the coupled Chua circuits (36). Different gray tones designate distinct periods of the driven subsystem. In fact, the diagram was computed with a help of the Poincaré section construction. Numbers in the gray areas indicate a number of cross-sections of the Poincaré surface per one entire period of the orbit. Bicritical point on the chart is marked with letter B. A rectangular fragment of the diagram near the bicritical point is shown in the inset, and then once more with magnification by factors  $\delta_1 = 4.6692\dots$  and  $\delta_2 = 2.3927\dots$  for the axes  $\alpha_1$  and  $\alpha_2$ , respectively. Observe good correspondence of the pictures and twofold increase of characteristic period for all dynamical regimes in the areas shown in the second inset in comparison with those in the first one.

**Table III. Main multipliers of periodic orbits at the bicritical point of two Chua's systems with unidirectional coupling**  
 $\alpha_1 = 6.542725993$ ,  $\alpha_2 = 6.64680875$ ,  $b = 10$ ,  $\varepsilon = 0.2$

$p=2^k$	$\mu$	$P=2^k$	$\mu$
2	-1.172447	64	-1.174172
4	-1.159058	128	-1.182497
8	-1.178773	256	-1.176030
16	-1.173025	512	-1.182088
32	-1.182463	1024	-1.178883

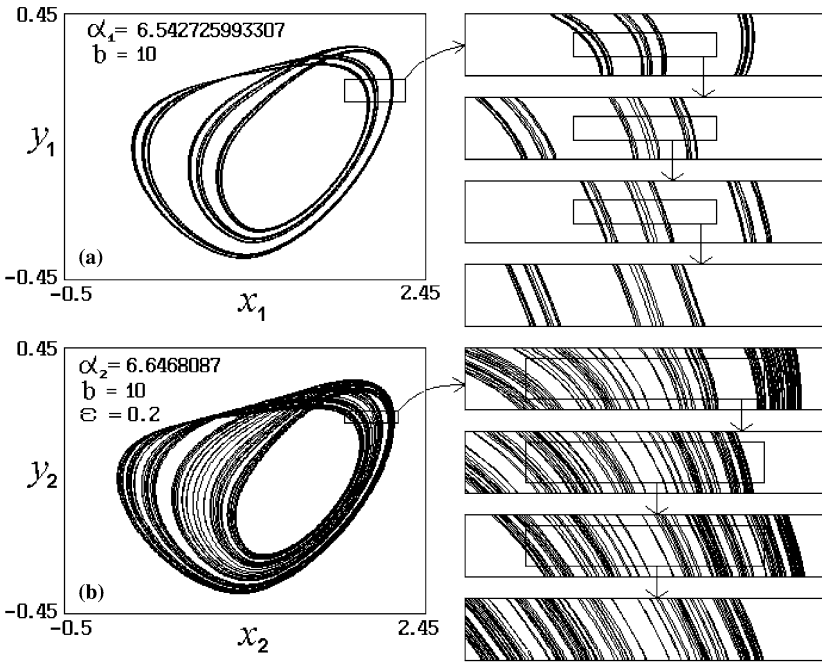


Fig. 12. Portraits of the bicritical attractors for the unidirectionally coupled Chua circuits in projections onto phase planes of the first (a) and of the second (b) subsystems. The right-hand panels represent fragments of the critical attractor with higher resolution. The magnification factor for the sequence of the fragments in the panel (a) is  $|\alpha| = 2.5029$ , and in panel (b)  $|\beta| = 1.5053$ .

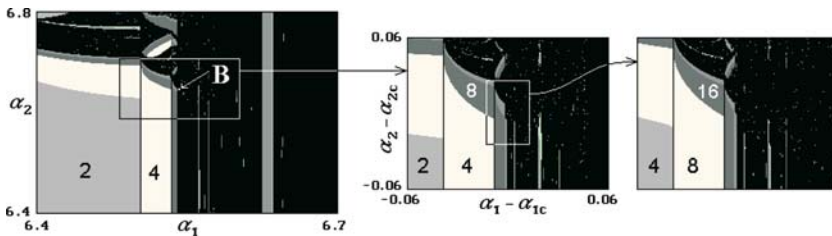


Fig. 13. Parameter plane  $(\alpha_1, \alpha_2)$  for the system of two Chua's circuits with unidirectional coupling. Gray tones designate distinct periods of the driven subsystem; numbers in the gray areas indicate a number of cross-sections of the Poincaré surface per a complete period of the motion. Black designates chaos or higher-period regimes. Near the bicritical point marked B a universal topography of regimes takes place, which reproduces itself under magnification by factors  $\delta_1 = 4.6692$  and  $\delta_2 = 2.3927$  along horizontal and vertical directions, as shown in insets.

### 4.3. Towards Observation of Criticality of FQ-type

In general, it is not so easy to locate a critical situation of FQ type in parameter space of a nonlinear system because of codimension 3. However, it is possible to construct some models, in which one can reach such critical point by variation of only two control parameters. For example, in the first work reported about the FQ critical behavior,<sup>(56)</sup> it was found in a system of two asymmetrically coupled one-dimensional maps

$$\begin{aligned}x_{n+1} &= 1 - \lambda x_n^2 - C y_n^2, \\y_{n+1} &= 1 - A y_n^2 - B x_n^2\end{aligned}\tag{37}$$

by variation of  $\lambda$  and  $A$  with fixed  $B$  and  $C$ . Apparently, it is so because coupling in the equations introduced via the quadratic terms is of dissipative type.<sup>8</sup> It is essential, however, that FQ criticality occurs in the case of *opposite signs of the coupling coefficients*  $B$  and  $C$ . Thus, one of the couplings must be associated with “negative dissipation”. In a physical realization, it means that the system would contain necessarily an active element (like negative resistor). In the model (37), for particular  $B=0.375$  and  $C=-0.25$  the FQ-point is placed at  $\lambda_c=1.654524590$ ,  $A=A_c=1.030837593$ , as computed in ref. 56.

On the same reasons as in the previous section, a more realistic model should be based on coupled two-dimensional invertible maps, say, Hénon-like maps, which may be interpreted as Poincaré maps for a hypothetical flow system. By analogy with coupled one-dimensional maps, we expect that the dissipative nature of coupling will be a condition of presence of the FQ criticality in a two-parameter family of the systems.

In ref. 57 the following form of dissipatively coupled Hénon-like maps was suggested:

$$\begin{aligned}x_{n+1} &= 1 - \lambda x_n^2 - C y_n^2 - b u_n + b C'(u_n - v_n), \\u_{n+1} &= x_n + C'(u_n - v_n), \\y_{n+1} &= 1 - A y_n^2 - B x_n^2 - b v_n + b B'(v_n - u_n), \\v_{n+1} &= y_n + B'(v_n - u_n),\end{aligned}\tag{38}$$

where  $B' = B(A - C)/(A\lambda - BC)$ ,  $C' = C(\lambda - B)/(A\lambda - BC)$ .

At fixed coupling coefficients  $B=0.375$ ,  $C=-0.25$  and at dissipation parameter  $b=0.3$ , a chart of the parameter plane  $(\lambda, A)$  is shown in the

<sup>8</sup>As we believe, dissipative nature of coupling corresponds to exclusion of the third eigenmode in linearized RG equation, presence of which would destroy a possibility of occurrence of the FQ criticality in a family of maps with two regulated parameters.

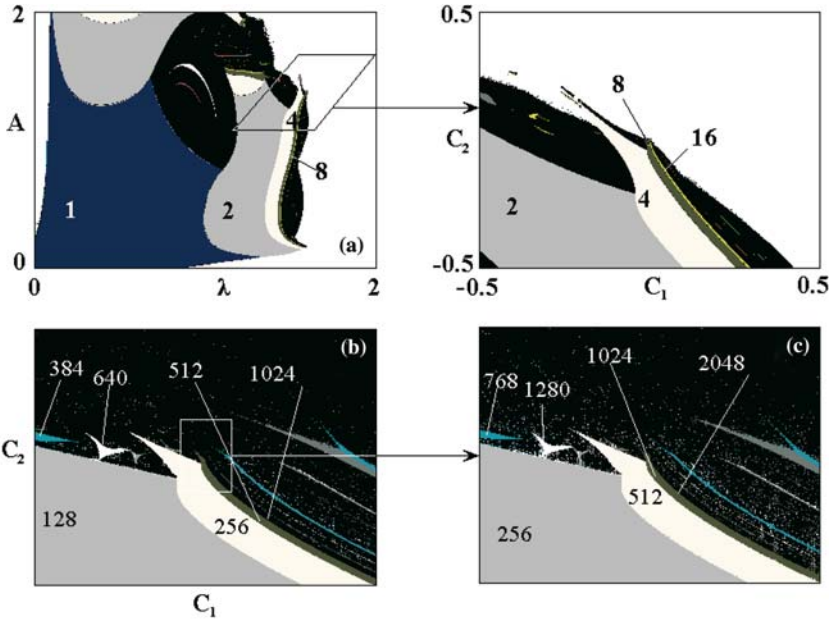


Fig. 14. Chart of dynamical regimes for the coupled Hénon maps (38) on the parameter plane  $(\lambda, A)$  at fixed  $B=0.375, C=-0.25, b=0.2$  (a). A neighborhood of the critical point FQ is shown separately in the inset in scaling coordinates  $A = A_c + C_2, \lambda = \lambda_c + C_1 + 0.8452C_2$ , where  $A_c$  and  $\lambda_c$  are coordinates of the critical point (39). Diagrams (b) and (c) demonstrate self-similarity of universal topography in a small vicinity of the critical point in respect to scale change with factors  $\delta_1=6.3263$  and  $\delta_2=3.4447$  along the horizontal and vertical axes, respectively.

first diagram of Fig. 14. One can see there a sequence of period-doubling bifurcation curves terminated on upper edges at some codimension-two bifurcation points, where two main multipliers become equal to  $(-1)$  for a respective period- $2^k$  orbit. Numerical estimate of the limit for the sequence of terminal points yields the critical point

$$\lambda = \lambda_c = 1.99689387746\dots, \quad A = A_c = 1.37271095406\dots \quad (39)$$

Is it a critical point of FQ type? In Table IV we present multipliers of unstable periodic orbits of period  $2^k$ . Observe that they demonstrate evident fast convergence to the universal values expected from the RG analysis. It indicates certainly affiliation of the critical point to the FQ universality class.

In Fig. 14a parameter plane  $(\lambda, A)$  is shown. Gray tones designate domains of different periods. Black corresponds to non-periodic regimes,

**Table IV. Multipliers of period- $p$  cycles at the critical point FQ in the coupled Hénon maps (38)  $\lambda = 1.99689387746$ ,  $A = 1.37271095406$ ,  $B = 0.375$ ,  $C = -0.25$**

$p = 2^k$	$\mu_1$	$\mu_2$
4	-1.598516	-1.264022
8	-1.614100	-1.102840
16	-1.613152	-1.019406
32	-1.583516	-1.047357
64	-1.571140	-1.077544
128	-1.588789	-1.049397
256	-1.583506	-1.042284
512	-1.574441	-1.060960
RG	-1.579739	-1.057149

including quasiperiodicity and chaos, and white to divergence of iterations to infinity. To demonstrate scaling properties of the parameter plane in a neighborhood of the critical point, an appropriate scaling coordinate system ( $C_1, C_2$ ) has to be introduced. It has been determined from computations in ref. 57 (see formula in the figure caption). A small parallelogram in Fig. 14a has sides directed along the axes of the scaling coordinate system. The coordinate axes  $C_1$  and  $C_2$  are associated with shifts from the critical point giving rise to the eigenmodes of the linearized RG equation with eigenvalues  $\delta_1$  and  $\delta_2$ , respectively. Topography of domains of different dynamical regimes inside this parallelogram is depicted in the inset in scaling coordinates. Diagrams (b) and (c) show yet smaller vicinities of the critical point in scaling coordinates to demonstrate the universal arrangement and local scaling properties of the parameter plane near the FQ point. In diagram (c) magnification in comparison with (b) is increased by factors  $\delta_1$  and  $\delta_2$  along the horizontal and the vertical axis, respectively. (See Fig. 3 for comparison.)

The above example proves that FQ criticality may be observed in systems like coupled driven dissipative nonlinear oscillators if the coupling is chosen in a right way. Indeed, in this case description in terms of the stroboscopic Poincaré map is appropriate. Both subsystems cross the fixed-time plane in the extended phase space simultaneously, so the problem reduces to that for coupled invertible two-dimensional maps of the same sort as the discussed Hénon map model (38).

What happens if we try to build up a system of two coupled *autonomous* self-oscillators? In the case of three-dimensional partial systems, the formally constructed Poincaré map is five-dimensional, not reducible, in general, to two coupled two-dimensional maps. Apparently, presence of



an additional dimension in the Poincaré map facilitates appearance of the third eigenmode in the solution of the RG equation, and it becomes necessary to have three control parameters to reach the critical situation FQ. A concrete example we have considered supports this assertion. This is a system of two Chua's circuits with dissipative coupling governed by equations

$$\begin{aligned} \dot{x}_1 &= \alpha_1 (y_1 - h(x_1)) + \varepsilon_1 (x_2 - x_1), & \dot{x}_2 &= \alpha_2 (y_2 - h(x_2)) + \varepsilon_2 (x_1 - x_2), \\ \dot{y}_1 &= x_1 + y_1 - z_1 + \varepsilon_1 (y_2 - y_1), & \dot{y}_2 &= x_2 + y_2 - z_2 + \varepsilon_2 (y_1 - y_2), \\ \dot{z}_1 &= -b_1 y_1 + \varepsilon_1 (z_2 - z_1), & \dot{z}_2 &= -b_2 y_2 + \varepsilon_2 (z_1 - z_2), \end{aligned} \quad (40)$$

$$h(x) = \begin{cases} (2x + 3)/7, & x \leq -1, \\ -x/7, & -1 < x < 1, \\ (2x - 3)/7, & x \geq 1. \end{cases}$$

A search for the FQ point by variation of only two parameters was unsuccessful. On the other hand, by variation of three parameters,  $\alpha_1$ ,  $\alpha_2$ , and  $b_1$  at fixed  $\varepsilon_1 = -0.05$ ,  $\varepsilon_2 = 0.2$ ,  $b_2 = 10$ , the FQ point was detected and located at

$$\begin{aligned} \alpha_1 &= 6.330061623840\dots, & \alpha_2 &= 6.585930638394\dots, \\ b_1 &= 10.19802309657\dots \end{aligned} \quad (41)$$

Table V gives evidence of the true FQ nature of this point. There we present pairs of largest in modulus multipliers for unstable periodic orbits coexisting at the critical point;  $p=2^k$  designates a number of steps of the Poincaré map necessary to close the cycle. Observe evident convergence to the universal values obtained from the RG analysis.

Figure 15 demonstrates another characteristic property of the FQ critical dynamics. It shows a portrait of the critical attractor of the coupled Chua circuits (40) in projection onto the plane of two variables relating to the first partial system,  $x_1$  and  $y_1$ . A fragment of the picture inside a small rectangular is magnified, and the series of pictures demonstrates in more details the fractal-like "strips" constituting the critical attractor. Under magnification by  $\alpha_1 = -1.9000\dots$  structure of the "strips" reproduces itself in accordance with our expectations based on the results of the RG analysis.<sup>9</sup>

<sup>9</sup>It is rather difficult to extract another scaling factor  $\beta = -4.0081\dots$  from such computations because of fast shrinking of the respective details of the fractal critical attractor.

**Table V. Multipliers of period- $p$  cycles at the critical point FQ in the coupled Chua circuits (40)  $\alpha_1 = 6.330061623840$ ,  $\alpha_2 = 6.585930638394$ ,  $b_1 = 10.19802309657$ ,  $b_2 = 10$ ,  $\varepsilon_1 = -0.05$ ,  $\varepsilon_2 = 0.2$**

$p = 2^k$	$\mu_1$	$\mu_2$
2	-1.608889	-1.060549
4	-1.611282	-1.022946
8	-1.593053	-1.037003
16	-1.557415	-1.086792
32	-1.586435	-1.067858
64	-1.594082	-1.025180
128	-1.562911	-1.078976
256	-1.579819	-1.057080
512	-1.558385	-1.071767
RG	-1.579739	-1.057149

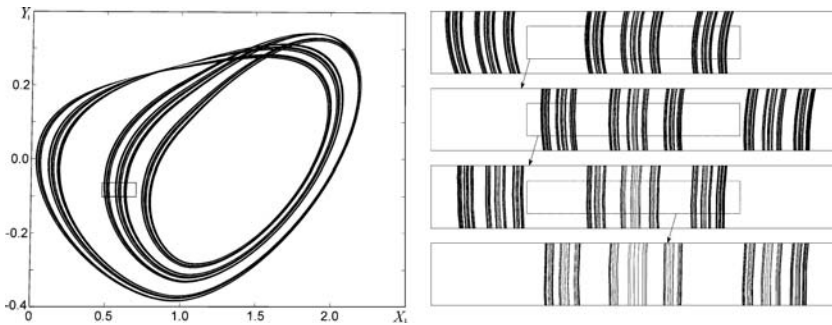


Fig. 15. Portrait of critical attractor of the coupled Chua circuits (40) at the point FQ in projection onto the plane of two variables relating to the first partial system. A small fragment of the picture inside a small rectangular is shown separately. Under subsequent magnification by factor  $|\alpha| = 1.9000\dots$  the structure of “strips” constituting the attractor reproduces itself on each second step of enlargement (account negative sign of  $\alpha$ ).

#### 4.4. Examples of Criticality of C-type and of Critical Quasi-Attractors

Let us turn to discussion of possibilities of observation of the critical behavior of C-type. In analogy with Section 3.4, where a non-invertible two-dimensional map was considered, we expect to meet the C-type criticality in a wide class of system in a situation, when variation of one parameter gives rise to period doublings, and variation of another one to a saddle-node bifurcation. Here we will consider two examples, one relates

to a problem of synchronization of a self-oscillating period-doubling system, and another to behavior at the edge of synchronization tongue near the bifurcation of Neimark–Sacker.

Our first example is a Rössler system under external periodic driving:

$$\dot{x} = -y - z + A \sin 2\pi \Omega t, \quad \dot{y} = x + ay, \quad \dot{z} = b + z(x - r), \quad (42)$$

where  $A$  and  $\Omega$  designate amplitude and frequency of the external force, and other parameters  $a$ ,  $b$ ,  $r$  are internal characteristics of the Rössler oscillator.

In a definite domain of the internal parameters, where the autonomous Rössler oscillator manifests periodic self-oscillations (the limit cycle), a supplement of the external force gives rise to synchronization (if the driving frequency is close to the frequency of self-oscillations) or to quasiperiodic beating (if the frequency difference is large enough). In Fig. 16 we show a picture of domains of different regimes in the parameter space  $(r, \Omega, A)$  as obtained in computations at fixed  $a = b = 0.2$ .<sup>(58)</sup> In a cross-section by a plane  $r = \text{const}$  the region of synchronization has a form of tongue, traditionally called the Arnold tongue. In the three-dimensional parameter space, the synchronization domain is bounded by two surfaces of the saddle-node bifurcations.

Let us increase the internal parameter  $r$ . In the autonomous Rössler system it gives rise to the period doubling bifurcation cascade. Inside the synchronization domain, the period-doubling bifurcations take place in the non-autonomous system as well. In the three-dimensional parameter space  $(r, \Omega, A)$ , they occur on definite surfaces, which accumulate to a limit, the Feigenbaum critical surface. Each of the period-doubling bifurcation surfaces has an edge line at the intersection with the boundary of the Arnold tongue. These lines are denoted in Fig. 16 as terminal curves.

The terminal curves corresponding to the subsequent period doublings converge to a limit, the curve of C-type criticality. As we know, in general, in the case of this critical behavior, the universal quantitative regularities start to act well only after a large number of the period-doubling bifurcations because of the slow convergence, due to presence of the eigenvalue  $\delta_3 \approx 0.93$  in the spectrum of the linearized RG transformation. Contribution of the slow mode may be excluded by a special selection of an additional parameter. In the system under consideration, we have found the point on the critical curve C optimal in a sense of convergence rate by careful selection of the driving amplitude  $A$ . In Fig. 16 it is marked with a bullet and, in accordance with numerical computations of ref. 58, has the following coordinates:

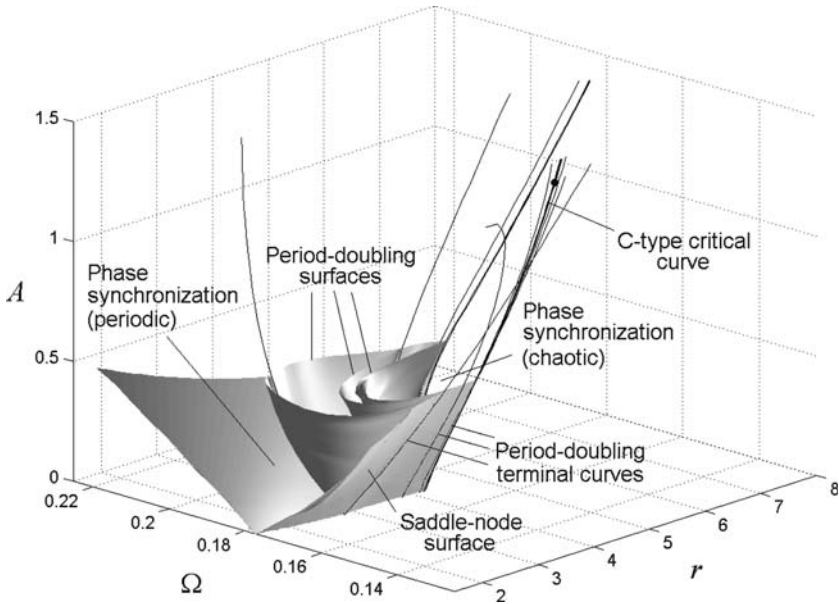


Fig. 16. 3D view of the parameter space  $(\Omega, r, A)$  for the periodically driven Rössler oscillator at  $a=b=0.2$ . The inscriptions explain nature of regimes and bifurcations. For clarity of the diagram, the bifurcational surfaces are drawn only partially. An optimal point for observation of the scaling regularities on the C-type critical curve is marked by a bullet.

$$r = 4.935701677\dots, \quad \Omega = 0.148253488\dots, \quad A = 1.35. \quad (43)$$

In Table VI the data for periodic orbits (stable and unstable) at the critical point are presented. Observe that the multipliers of the periodic orbits are in good correspondence with the expected universal values (see the last row in the Table).

A remarkable feature of dynamics at the critical point C derived from the RG analysis is presence of *the critical quasiattractor*, a countable infinite set of coexisting stable cycles of period proportional to  $4^k$ ,  $k=0, 1, 2, \dots$ . In computations, it is possible to get at least several first representatives of this family of attractors. Their phase portraits are shown in Fig. 17.

As known, the Rössler oscillator manifests dynamical behavior typical for a wide class of low-dimensional dissipative chaotic systems, namely, the period-doubling cascade and the birth of a chaotic attractor of spiral type. We believe that dynamical properties analogous to those found in the forced Rössler oscillator will occur also in other systems of this

**Table VI. Multipliers of cycles of period of  $p$  units of the driving period at the critical point of C type in the driven Rössler oscillator  $r=4.935701677$ ,  $=0.148253488$ ,  $A=1.35$**

$p=4^k$	$\mu_2^{(1)}$	$\mu_1^{(1)}$	$p=2 \cdot 4^k$	$\mu_2^{(2)}$	$\mu_1^{(2)}$
1	0.777162	-0.600727	2	1.229085	-0.911129
4	0.858520	-0.685901	8	1.180212	-0.860374
16	0.85021	-0.71942	32	1.17467	-0.84945
64	0.84756	-0.73033	128	1.1724	-0.8342
256	0.850	-0.721			
RG	0.847450	-0.725255	RG	1.174459	-0.848865

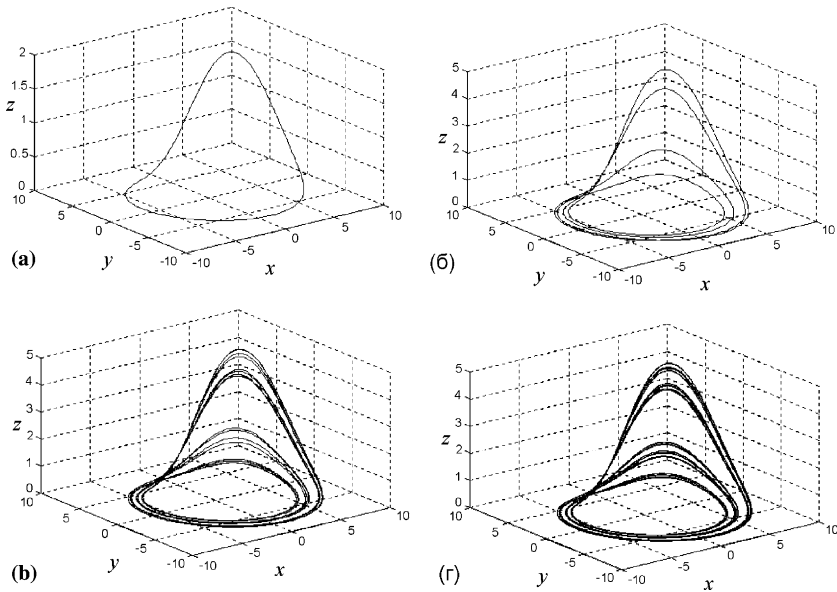


Fig. 17. Attractive limit cycles of period 1 (a), 4 (b), 16 (c), and 64 (d) (measured in units of the period of external force) for the periodically driven Rössler oscillator at the critical point (43). These are four representatives of an infinite set of stable periodic orbits constituting the critical quasiattractor.

class under external periodic driving. It may be expected that the critical behavior of C-type could be observed in carefully organized experiments on synchronization of period doubling dissipative systems (e.g. convective systems, electronic oscillators, etc.). As may be conjectured, this is a universal attribute of the synchronization breakup corresponding to the limit of period-doubling at the edge of Arnold tongue. Of course, in

experiments only a finite number of the stable orbits from the critical quasi-attractor will be observable.

Let us turn to another example. As we believe, it is of principal significance, although relates to an artificially constructed model map.

One of the most widely discussed scenarios of the onset of turbulence comes back to Landau and Hopf<sup>(59,60)</sup> and consists, as they suggested, in subsequent birth of oscillatory components with incommensurate frequencies, or, in language of more modern nonlinear dynamics, in subsequent birth of attractors represented by tori of higher and higher dimensions. In accordance with latter argumentation of Ruelle and Takens,<sup>(61)</sup> after few first bifurcations a strange chaotic attractor will be born instead of the higher-dimensional torus. In any case, this picture contains an intermediate stage of bifurcation of the onset of torus from the limit cycle. It is known as the bifurcation of Neimark–Sacker.<sup>(27,28)</sup>

Let us construct a model map, which can demonstrate all bifurcations relevant for the problem of stability loss of a limit cycle, including the Neimark–Sacker bifurcation.

In linear stability analysis of dynamics in terms of Poincaré section near a limit cycle one obtains a linear map, which may be written in appropriately chosen variables as

$$x_{n+1} = Sx_n - y_n, \quad y_{n+1} = Jx_n, \quad (44)$$

where  $S$  and  $J$  are trace and determinant of the Jacobian matrix defined over one period of the cycle. They depend in some way on parameters of the problem, but here we prefer to regard  $S$  and  $J$  themselves as control parameters. The Floquet eigenvalues, or multipliers, are the roots of the quadratic equation  $\mu^2 - S\mu + J = 0$ . Domain of stability of the limit cycle is determined by condition that both multipliers are less than one in modulus. On the parameter plane  $(S, J)$  it is a triangle with sides

- $1 - S + J = 0$  (one multiplier equals 1),
- $1 + S + J = 0$  (one multiplier equals  $-1$ ), and
- $J = 1$  (two complex conjugate multipliers have unit modulus)

(see Fig. 18a and refs. 62, 63).

Next, we introduce nonlinearity “by hands”, in a hope that the most common features of the bifurcation transitions will be caught in the constructed map. Namely, we set<sup>(64)</sup>

$$x_{n+1} = Sx_n - y_n - (\varepsilon y_n^2 + x_n^2), \quad y_{n+1} = Jx_n - (y_n^2 + x_n^2)/5. \quad (45)$$

In Fig. 18b we present chart of dynamical regimes for the map (45) on the parameter plane  $(S, J)$  at fixed  $\varepsilon = 0.535$ . One easily recognizes the stability triangle. Inside of it, attractor is a fixed point at the origin. On the left side, it undergoes the period-doubling bifurcation, and subsequent bifurcations of the period-doubling cascade may be seen as well. On the right side (dashed line), a saddle-node bifurcation happens accompanied with a jump to another fixed-point attractor, which can undergo its own bifurcations. On the topside, the Neimark–Sacker bifurcation takes place of birth of motion spiraling around the former attractive fixed point. Concrete nature of a regime depends on the rotational number linked with argument of the complex multiplier at the bifurcation. In the region upper the bifurcation border one can see tongues of periodic regimes and domains of quasiperiodicity between them.

Let us consider in more details one of the tongues, that of period 4. Diagram (c) shows this tongue and its neighborhood with magnification. Observe that the period-doubling bifurcation curves inside the tongue visibly stick into the edge. Computations confirm that there is a sequence of terminal points for the period-doubling bifurcation curves at the edge of the synchronization tongue, which converges to a limit point located at

$$S = S_c = -0.548966 \dots, \quad J = J_c = 1.547188 \dots \tag{46}$$

This is a critical point of C-type. To give evidence of its nature on the quantitative level, we present in Table VII numerical data on multipliers for cycles of period  $2^k$  computed at this point.

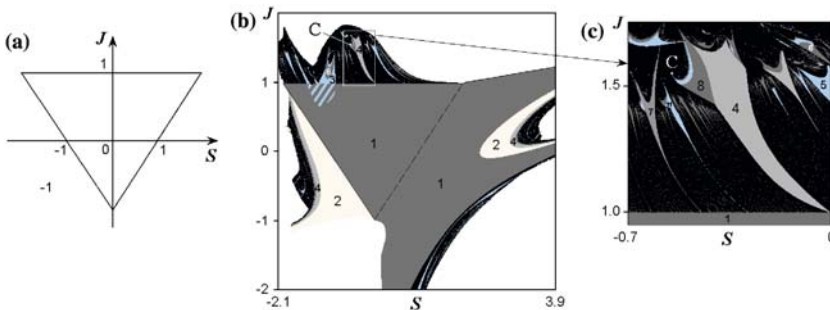


Fig. 18. Parameter plane for the model map (45): (a) triangle of stability for the fixed point at origin; (b) chart of dynamical regimes and its magnified fragment (c). Gray scales are used to show areas of periodic dynamics. Black designate chaos, quasiperiodicity or unrecognized high-period regimes. Stripped area indicates coexistence of different attractors. Critical point C located at the period-doubling accumulation point at the edge of synchronization tongue is marked in diagrams (b) and (c).

Observe nice correspondence of multipliers to the universal values known from the RG analysis (the last row of the Table). A fast convergence to the universal constants occurs because we exclude contribution from the slow decaying mode of the RG equation by special selection of  $\varepsilon$ .

As we found, critical points of the same nature occur inside some other tongues above the Neimark–Sacker bifurcation.

As follows from this example, in the multiparameter analysis of transition to turbulence via quasiperiodicity (scenario of Landau–Hopf–Ruelle–Takens), already on a stage of birth of the second incommensurate frequency, one can expect presence of critical points of C-type with intrinsic nontrivial features of dynamical behavior, including coexistence of a countable set of attractive periodic orbits.

## 5. CONCLUSION AND GENERAL DISCUSSION

In many fields of mathematics, researchers use to classify entities according to their codimension, which may be thought as a number of parameters adjusted to observe the phenomenon. In particular, this approach is of fundamental significance in bifurcation theory and catastrophe theory. After Feigenbaum’s discovery of the period-doubling universality and development of the renormalization-group (RG) method, it seems natural in this spirit to turn to search and classification for situations, which can occur in multiparameter analysis of the onset of chaos and allow the RG analysis.<sup>(31,65,66)</sup> We call this field *a theory of multiparameter criticality*.

In this paper we concern only a part of this broad area, namely, we outline situations linked with period-doubling transitions to chaos with a second phase-space dimension coming into play. It requires using at least two-dimensional maps as the simplest representatives for the universality classes. Each type of critical behavior corresponds to a fixed-point or a periodic solution of the two-dimensional generalization of Feigenbaum-

**Table VII. Multipliers of cycles of period  $p$  at the critical point of C type in the model map (45)  $S = -0.548966$ ,  $J = 1.547188$ ,  $\varepsilon = 0.535$**

$p = 4^k$	$\mu_2^{(2)}$	$\mu_1^{(2)}$	$p = 2 \cdot 4^k$	$\mu_2^{(1)}$	$\mu_1^{(1)}$
64	1.179719	-0.874220	128	0.859691	-0.695732
256	1.175752	-0.855538	512	0.850658	-0.722936
512	1.172441	-0.847454	2048	0.847450	-0.725255
RG	1.174459	-0.848865	RG	0.847450	-0.725255



Cvitanović equation and is characterized by a set of universal constants, like Feigenbaum's  $\alpha$  and  $\delta$ . We present a number of realistic systems manifesting those types of critical behavior and indicate some relevant conditions for their possible observation in physical experiments.

Concretely, we discussed four types of criticality:

- H-type, which was discovered in the context of conservative period doubling, but occurs as well in dissipative dynamics, as a phenomenon of codimension 2;
- bicritical behavior, which occurs in systems allowing decomposition onto two unidirectionally coupled dissipative period-doubling subsystems, each of which is brought by parameter tuning onto the threshold of chaos;
- FQ-type, which takes place in a degenerate class of two-dimensional maps, represented in appropriate coordinates via functions of combinations  $X^2$  and  $XY$ ;
- C-type, which occurs in noninvertible two-dimensional maps represented as a composition of a fold mapping with a general affine transformation; it is associated with a period-2 saddle solution of the RG equation.

We have indicated a novel possibility for realization of the H type criticality that consists not in a trivial reduction of dissipation, but in compensation of it in a self-oscillatory system. For bicriticality, we have presented a number of examples, e.g. coupled Hénon-like maps, coupled driven oscillators, coupled chaotic self-oscillators, which manifest this type of behavior. For FQ-type we indicate possibility to arrange it in non-symmetric systems of coupled period-doubling subsystems, e.g. Hénon-like maps and Chua's circuits. For C-type we present examples of its appearance in a driven Rössler oscillator at the period-doubling accumulation on the edge of synchronization tongue and in a model map with the Neimark-Sacker bifurcation.

An alternative possibility for appearance of non-Feigenbaum critical behavior relates to a case when the dynamics at the period-doubling onset of chaos remains essentially one-dimensional, but the one-dimensional map is distorted in such degree that leaves the Feigenbaum universality class.

To give a very short summary of related results, we remind that soon after Feigenbaum's works it was noted that qualitatively the same period doubling bifurcation cascade occurs in maps like  $x_{n+1} = 1 - \lambda|x|^\kappa$ , where  $\kappa > 1$  is a real constant. It appears that factors  $\alpha$  and  $\delta$  depend on  $\kappa$ .<sup>(67-69)</sup> RG analysis of this case gives rise to a family of fixed-point solutions

of the Feigenbaum-Cvitanović equation represented as expansions over powers of  $|x|^\kappa$ .

Arbitrary degree of extremum in a one-dimensional map is not a pure academic subject, but occurs in the context of the so-called homoclinic bifurcations in flow systems. It relates to the onset of chaos due to formation of a homoclinic structure associated with a saddle point in the phase space. In description in terms of the Poincaré map with approximation by a one-dimensional map, degree of the extremum  $\kappa$  is linked with a ratio of eigenvalues of the saddle point.<sup>(65,70–72)</sup> It is worth noting a remarkable fact of existence of nontrivial limit behavior for universal constants at  $\kappa \rightarrow \infty$ . (In particular,  $\delta$  converges to 27.576303.<sup>(73,74)</sup>)

In addition, there is a number of publications devoted to period doubling cascades in unimodal maps possessing a degree- $\kappa$  maximum with differing left and right  $\kappa$ th derivatives controlled by two parameters.<sup>(75–77)</sup> In RG analysis, the critical situation at the chaos threshold is associated with period-2 solutions of the Feigenbaum–Cvitanović equation. The case of differing left- and right-hand degrees was also discussed.<sup>(78)</sup>

Recently, in ref. 79 a phenomenon was studied consisting in disappearance of period-doubling cascades due to collision of the periodic orbits with a saddle-type equilibrium point. It corresponds to some special critical situation in flow systems that occurs in a two-parameter analysis, referred to as the homoclinic doubling cascade. As shown, this phenomenon possesses some scaling regularities and may be analyzed on a basis of model one-dimensional maps representing the universality class.

If we restrict ourselves with apparently a more natural case of smooth analytic maps, the degree of extremum has to be an even integer, e.g.  $\kappa = 2, 4, 6, \dots$ . Quadratic extremum corresponds to the Feigenbaum universality class. The next  $\kappa = 4$  corresponds to the so-called tricritical points.<sup>(51,80–83)</sup>

In a family of unimodal one-dimensional maps the tricriticality occurs as a phenomenon of codimension 3. (Two parameters are necessary to ensure vanishing the second and the third derivatives at the extremum point, and one more to control the period-doubling bifurcation cascade under the imposed condition.)

Alternatively, one can get the tricritical situation in a two-parameter family of one-dimensional maps with two extrema called the bimodal maps. In this case, a curve may exist on the parameter plane determined by a requirement that one extremum is mapped precisely to another. Then, as iterated map accepts a quartic extremum, and the period-doubling cascade, if occurs, gives rise to the tricritical point. On the parameter plane, such tricritical points appear as terminal points of pieces of Feigenbaum's critical lines.<sup>(80,81)</sup>

Passage from one-dimensional maps to Hénon-like two-dimensional dissipative maps does not destroy the tricriticality of codimension 3, but, the tricriticality of codimension 2, in contrast, does not survive.<sup>(82)</sup> Sometimes a number of the period-doublings needed to notice a deflection from the true tricritical regularities is large enough. It may happen that it can be impossible to detect any difference with true tricriticality in any thinkable experiment, or even in computations of commonly used double precision. In such cases, the tricritical scaling occurs as a kind of intermediate asymptotics valid for a number of observable period-doubling levels, and we speak of the pseudo-tricritical behavior (see examples in refs. 51, 83).

In bimodal maps, as follows from two-parameter analysis the border of chaos on the parameter plane is of complex nature.<sup>(55,81,84,85)</sup> It contains fragments of Feigenbaum critical lines and an infinite fractal-like set of critical points of codimension 2. They may be regarded as period-doubling accumulation points on a set of paths in the parameter plane, which form a binary tree. These critical points are in one-to-one correspondence with a set of binary codes determining all possible itineraries on the tree. Tricritical points are particular representatives of this set with codes containing a tail of one repetitive definite symbol. Critical points with tails of codes determined by repetitive fragments of  $p$  symbols are associated with cycles of the Feigenbaum–Cvitanović equation of the period  $p$ . It means that structures in phase space and in parameter space manifest self-similarity after each  $p$  steps of the doubling transformation. Non-periodic codes correspond to non-periodic orbits of the RG equation, and in this case one can speak about scaling only in statistical sense (the so-called *renormalization chaos*). As demonstrated in computations, critical points with periodic codes, not relating to the tricritical class, survive with passage to the Hénon-like maps.<sup>(86,83)</sup>

A clear indicator of the outlined picture of critical behavior intrinsic to bimodal maps visible in parameter planes of many realistic systems, is presence of structures called “crossroad area”, “swallows”, and “shrimps”.<sup>(87–89)</sup>

Situations of appearance of higher degrees of extrema under iterations of smooth one-dimensional maps are possible as well.<sup>(90)</sup> In particular, a critical behavior corresponding to an extremum of the 6-th power takes place if a map has a quadratic extremum and a cubic inflection point, and one is mapped to another. This may occur generically on a curve in a three-dimensional parameter space. If the period-doubling bifurcation cascade takes place along this curve, the accumulation yields the critical point of the respective class. In a case of three quadratic extrema, the first mapped to the second, and the second to the third, the iterated map accepts extremum of the 8-th power. Again, this situation is generic

on a curve in a three-dimensional parameter space, so the critical point of period-doubling accumulation of this type may appear as a phenomenon of codimension 3.

A number of universality classes was found in complex analytical (conformal) iterative maps. They may be equivalently represented as real two-dimensional maps satisfying the Cauchy–Riemann equations. In complex maps of degree 3, 4, 5, 6, ... the period-doubling cascades occur represented by converging sequences of bifurcation points on the complex parameter plane. Complex solutions of the Feigenbaum-Cvitanović equation corresponding to the limit points of these cascades were obtained and universal complex constants  $\alpha$  and  $\delta$  estimated.<sup>(91–93)</sup> For complex quadratic map, beside the period doubling on the real axis, cascades of period tripling, quadrupling, etc. in the complex parameter plane take place.<sup>(94,95)</sup> The respective critical points are particular points of the well-known Mandelbrot set.<sup>(96)</sup> In the class of analytic maps, the critical points of accumulation of the  $m$ -tupling bifurcation cascades are of codimension 2. It corresponds to presence of a single complex eigenvalue of the linearized equation near the complex fixed-point of the  $m$ -tupling RG transformation. For the case of period-tripling it was shown that in a class of general smooth two-dimensional maps (not satisfying necessarily the Cauchy–Riemann equations) an additional relevant complex eigenvalue appears. As follows, the period-tripling accumulation point for these maps is of codimension 4.<sup>(97)</sup>

In concern with the conservative period-doubling, beside the mentioned H type of criticality, universal regularities intrinsic to four-dimensional symplectic maps were studied.<sup>(98,99)</sup>

Another range of questions in the field of multi-parameter criticality relates to the quasiperiodic dynamics. Here, the starting point is a codimension-2 critical situation known after Shenker,<sup>(100)</sup> which occurs at the golden-mean rotational number in the sine circle map having a cubic inflection point. Renormalization group analysis was developed in early 80th.<sup>(101,102)</sup> This critical situation was found in two-dimensional maps,<sup>(103)</sup> in forced nonlinear oscillators,<sup>(16)</sup> in experiments with fluid convection<sup>(104)</sup> and with electronic circuits.<sup>(105,106)</sup> Also, some regularities were stated embracing the complete set of rotational numbers, and attempts of description in terms of RG approach were undertaken.<sup>(107,108)</sup> In addition, more complicated situations of inflection points of higher order or presence of more than one inflection points on the basic interval were analyzed.<sup>(109–111)</sup>

A conservative version of the critical quasiperiodic dynamics appears in a problem of destruction of the Kolmogorov–Arnold–Moser tori. As believed, the last torus is that of the golden-mean rotational number. RG

analysis for this case was developed in refs. 112–115. In addition, critical situations of higher codimension were distinguished and studied.<sup>(116–118)</sup> Some results are known for other rotational numbers, including renormalization chaos, corresponding to non-periodic behavior of solutions under iterations of the RG transformation.<sup>(119,120)</sup>

In the context of quasiperiodicity, it is worth mentioning a research direction concerning application of the RG approach to situations of birth of strange nonchaotic attractors.<sup>(121)</sup> For several critical situations (a blow-out bifurcation, terminal points of bifurcations of torus doubling and torus collision, a critical point separating situations of smooth and fractal tori collision) formulation of the respective functional equations, their numerical solution, estimates of universal constants, study of local parameter space topography were presented in refs. 122–125.

Finally, we have to mention transitions via intermittency. The most common kind of intermittency introduced by Pomeau and Manneville (type I), is characterized by alternating stages of relatively long “laminar” stages and relatively short “turbulent” ones.<sup>(126)</sup> The laminar stages correspond to travel of the orbit through a narrow “channel” arising after bifurcation of collision and disappearance of a pair of fixed points (or periodic orbits), one stable and another unstable. In the critical situation, duration of the laminar phases approaches infinity. Several versions of the RG analysis were suggested relating to the laminar stage dynamics.<sup>(127–129)</sup> One of them exactly repeats the Feigenbaum–Cvitanović analysis, but the solution of the functional equation relates to a distinct class of functions (fractional-linear maps) and is obtained in an explicit analytic form. Analogous theory was developed for type-III intermittency, for laminar stages corresponding to dynamics near the subcritical period-doubling bifurcation.<sup>(130)</sup>

For conservative systems intermittent critical behavior was revealed and studied similar to that of type I in dissipative case.<sup>(131,132)</sup> Moreover, Zisook has developed a generalized approach based on theory of singularities of differentiable maps and classified a number of universality classes for intermittency in conservative case.<sup>(133)</sup>

It may be expected that further development of the theory of multiparameter criticality will shed light onto universal behaviors of nonlinear systems in a course of transitions to multidimensional chaos. Models constructed as the simplest representatives of the universality classes will be useful for phenomenological quantitative description locally near the respective critical situations even in such cases, when dynamical equations are awkward or unknown. Unfortunately, beside the RG approach, we do not have now a general mathematical principle for distinguishing critical situations to be studied (in contrast to the bifurcation theory and

catastrophe theory). In many respects conclusions are based on numerical computations and plausible hypotheses rather than on rigorous mathematical considerations. Nevertheless, it is clear that the multi-parameter criticality must be regarded as important research direction in nonlinear dynamics, which has many significant achievements and promises deep and interesting developments.

The authors acknowledge support from RFBR grant No. 03-02-16074.

## REFERENCES

1. M. J. Feigenbaum, Quantitative universality for a class of nonlinear transformations, *J. Stat. Phys.* **19**:25–52 (1978).
2. M. J. Feigenbaum, The universal metric properties of nonlinear transformations, *J. Stat. Phys.* **21**:669–706 (1979).
3. P. Cvitanović (ed.), *Universality in Chaos*, 2nd Ed. (Adam Bilger, Boston, 1989).
4. P. Collet, J.-P. Eckmann, and H. Koch, Period Doubling Bifurcations for Families of Maps on  $\mathbb{R}^n$ , *J. Stat. Phys.* **25**:1–14 (1981).
5. E. B. Vul, Ya. G. Sinai, and K. M. Khanin, Feigenbaum universality and thermodynamic formalism, *Russ. Math. Surv.* **39**:1–40 (1984).
6. J. P. Crutchfield and B. A. Huberman, Fluctuations and the onset of chaos, *Phys. Lett. A* **77**:407–410 (1980).
7. A. J. Lichtenberg and M. A. Lieberman, *Regular and Chaotic Dynamics*, 2nd Edn. (Springer-Verlag, 1992).
8. J. A. C. Gallas, Structure of the parameter space of the Hénon map, *Phys. Rev. Lett.* **70**:2714–2717 (1993).
9. H. J. Carmichael, R. R. Snapp, and W. C. Schieve, Oscillatory instabilities leading to “optical turbulence” in a bistable ring cavity, *Phys. Rev. A* **26**:3408–3422 (1982).
10. L. Glass and R. Perez, Fine Structure of Phase Locking, *Phys. Rev. Lett.* **48**:1772–1775 (1982).
11. S. R. G. Novak, Fehlich Transition to chaos in the Duffing oscillator, *Phys. Rev. A* **26**:3660–3663 (1982).
12. W. Moon and P. J. Holmes, A magnetoelastic strange attractor, *J. Sound Vib.* **65**:285–296 (1979).
13. J. Testa, J. Perez, and C. Jeffries, Evidence for universal chaotic behavior of a driven nonlinear oscillator, *Phys. Rev. Lett.* **48**:714–717 (1982).
14. P. Beiersdorfer, J. M. Wersinger, Topology of the Invariant Manifolds of a Period-doubling Attractors for Some Forced Nonlinear Oscillators, *Phys. Lett. A* **96**:269–272 (1983).
15. M. Schanz and A. Pelster, On the Period-Doubling Scenario in Dynamical Systems with Time Delay, *Proceedings of the 15th IMACS World Congress 1997* **I**:215–220 (Wissenschaft and Technik, 1997).
16. V. S. Anishchenko, *Dynamical Chaos in Physical Systems: Experimental Investigation of Self-Oscillating Circuits* (World Sci. Publ. Singapore, 1989).
17. A. S. Dmitriev and V. Ya. Kislov, *Stochastic oscillations in radiophysics and electronics* (Moscow, Nauka, 1989). (In Russian.)
18. M. Komura, R. Tokunaga, T. Matsumoto, and L. O. Chua, Global bifurcation analysis of the double scroll circuit, *Int. J. Bifurcation Chaos* **1**:139–182 (1991).

19. N. M. Ryskin, V. N. Titov, and D. I. Trubetskov, Transition to the Chaotic Regime in a System Composed of an Electron Beam and an Inverse Electromagnetic Wave, *Doklady Physics* **43**:90–93 (1998).
20. J. Maurer and A. Libchaber, Rayleigh-Bénard experiment in liquid helium: frequency locking and the onset of turbulence, *J. de Physique Lettres* **40**:419–423 (1979).
21. A. Libchaber, C. Laroche, and S. Fauve, Period doubling in mercury, a quantitative measurement, *J. de Phys. Lett.* **43**:211–216 (1982).
22. W. Lauterborn, E. Schmitz, and A. Judt, Experimental approach to a complex acoustic system, *Int. J. Bifurcation Chaos* **3**:635–642 (1993).
23. F. T. Arecci, R. Meucci, G. Puccioni, and J. Tredicce, Experimental Evidence of Sub-harmonic Bifurcations, Multistability, and Turbulence in a Q-Switched Gas Laser, *Phys. Rev. Lett.* **49**:1217–1220 (1982).
24. R. Vallée and C. Delisle, Route to chaos in an acousto-optic bistable device, *Phys. Rev. A* **31**:2390–2396 (1985).
25. T. Poston and I. Stewart, *Catastrophe Theory and its Application* (Dover Publications, 1997).
26. V. I. Arnol'd and G. S. Wassermann, *Catastrophe Theory* (Springer-Verlag, 1992).
27. J. Guckenheimer and P. Holmes, *Nonlinear Oscillations, Dynamical Systems, and Bifurcations of Vector Fields* (Springer-Verlag, New York, 1997).
28. Y. A. Kuznetsov, *Elements of Applied Bifurcation Theory* (Springer-Verlag, New York, 1995).
29. J.-P. Eckmann, H. Koch, and P. Wittwer, Existence of a fixed point of the doubling transformation for area-preserving maps of the plane, *Phys. Rev. A* **26**:720–722 (1982).
30. G. R. W. Quispel, Universal functional equation for period doubling in constant-Jacobian maps, *Phys. Lett. A* **118**:457–462 (1986).
31. A. P. Kuznetsov, S. P. Kuznetsov and I. R. Sataev, A variety of period-doubling universality classes in multi-parameter analysis of transition to chaos, *Physica D* **109**:91–112 (1997). See also: <http://sgtnd.narod.ru/science/alphabet/eng/index.htm>.
32. R. S. MacKay, Period doubling as a universal route to stochasticity. In book: *Long time prediction in dynamics*, eds. W. Horton, L. E. Reichl, and V. Szebehely (J. Wiley & Sons, New York, 1983).
33. C. Chen, G. Gyorgyi, and G. Schmidt, Universal transition between Hamiltonian and dissipative chaos, *Phys. Rev. A* **34**:2568–2570 (1986).
34. J. M. Greene, R. S. MacKay, F. Vivaldi, and M. J. Feigenbaum, Universal behavior in families of area preserving maps, *Physica D* **3**:468–486 (1981).
35. M. Widom and L. P. Kadanoff, Renormalization group analysis of bifurcations in area-preserving maps, *Physica D* **5**:287–292 (1982).
36. J. F. Heagy, A physical interpretation of the Henon map, *Physica D* **57**:436–446 (1992).
37. C. Chen, G. Gyorgyi, and G. Schmidt, Universal scaling in dissipative systems, *Phys. Rev. A* **35**:2660–2668 (1987).
38. C. Reick, Universal corrections to parameter scaling in period-doubling systems: Multiple scaling and crossover, *Phys. Rev. A* **45**:777–792 (1992).
39. B. P. Bezruchko, Yu. V. Gulyaev, S. P. Kuznetsov, and E. P. Seleznev, New type of critical behavior of coupled systems at the transition to chaos, *Sov. Phys. Dokl.* **31**:258–260 (1986).
40. A. P. Kuznetsov, S. P. Kuznetsov, and I. R. Sataev, Bicritical dynamics of period-doubling systems with unidirectional coupling, *Int. J. Bifurcation Chaos* **1**:839–848 (1991).
41. K. Kaneko, Spatial period-doubling in open flow, *Phys. Lett. A* **111**:321–325 (1985).
42. I. S. Aranson, A. V. Gaponov-Grekhov, and M. I. Rabinovich, The onset and spatial development of turbulence in flow systems, *Physica D* **33**:1–20 (1988).

43. P. Philominathan and P. Neelamegam, Characterization of chaotic attractors at bifurcations in Murali-Lakshmanan-Chua's circuit and one-way coupled map lattice system, *Chaos, Soliton and Fractals* **12**:1005–1017 (2001).
44. T. Heil, J. Mulet, I. Fischer, C. R. Mirasso, M. Peil, P. Colet, and W. Elsäber, ON/OFF Phase Shift Keying for Chaos-Encrypted Communication Using External-Cavity Semiconductor Lasers, *IEEE J. Quant. Electronics* **38**:1162–1170 (2002).
45. S. Wang, J. Kuang, J. Li, Y. Luo, H. Lu and G. Hu, Chaos-based secure communications in a large community, *Phys. Rev. E* **66**:065202 (2002).
46. A. P. Kuznetsov, S. P. Kuznetsov, and I. R. Sataev, Variety of types of critical behavior and multistability in period doubling systems with unidirectional coupling near the onset of chaos, *Int. J. Bifurcation Chaos* **3**:139–152 (1993).
47. S. P. Kuznetsov and I. R. Sataev, Period-doubling for two-dimensional non-invertible maps: Renormalization group analysis and quantitative universality, *Physica D* **101**:249–269 (1997).
48. H. Whitney, On Singularities of Mappings of Euclidean Spaces. I. Mappings of the Plane into the Plane, *Ann. Math.* **62**:374–410 (1955).
49. K. Flensberg and H. Svensmark, Scaling relations for forced oscillators at the transition from a dissipative to a Hamiltonian system, *Phys. Rev. E* **47**:289–305 (1993).
50. S. P. Kuznetsov and A.S.Pikovsky, Universality and scaling of period-doubling bifurcations in a dissipative distributed medium, *Physica D* **19**:384–396 (1986).
51. A. P. Kuznetsov, S. P. Kuznetsov, I. R. Sataev, and L. O. Chua, Multi-parameter criticality in Chua's circuit at period-doubling transition to chaos, *Int. J. Bifurcation Chaos* **6**:119–148 (1996).
52. S.-Y. Kim and W. Lim, Bicritical scaling behavior in unidirectionally coupled oscillators, *Phys. Rev. E* **63**:036223 (2001).
53. A. Pikovsky, M. Rosenblum, and J. Kurths, *Synchronization. A universal concept in nonlinear sciences* (Cambridge Univ. Press, 2002).
54. M. Genot, Application of 1D Chua's map From Chua's circuit: A pictorial guide, *J. Circuits, Systems and Computers* **3**:431–440 (1993).
55. A. P. Kuznetsov, S. P. Kuznetsov, I. R. Sataev, and L. O. Chua, Two-parameter study of transition to chaos in Chua's circuit: renormalization group, universality and scaling, *Int. J. Bifurcation Chaos* **3**:943–962 (1993).
56. S. P. Kuznetsov and I. R. Sataev, New types of critical dynamics for two-dimensional maps, *Phys. Lett. A* **162**:236–242 (1992).
57. A. P. Kuznetsov, A. V. Savin, and S.-Y. Kim, On the Criticality of the FQ-Type in the System of Coupled Maps with Period-Doubling, *Nonlinear Phenomena in Complex Systems* **7**:69–77 (2004).
58. S. P. Kuznetsov and I. R. Sataev, Universality and scaling for the breakup of phase synchronization at the onset of chaos in a periodically driven Rössler oscillator, *Phys. Rev. E* **64**:046214 (2001).
59. L. D. Landau, On the problem of turbulence, *Doklady Akademii Nauk SSSR* **44**:311 (1944). (In Russian.)
60. E. Hopf, A mathematical example displaying features of turbulence, *Commun. Appl. Math.* **1**:303–322 (1948).
61. D. Ruelle and F. Takens, On the nature of turbulence, *Commun. Math. Phys.* **20**:167–192 (1971).
62. J. M. T. Thompson and H. B. Stewart, *Nonlinear Dynamics and Chaos. Geometrical Methods for Engineers and Scientists* (John Wiley and Sons, Chichester – NY – Brisbane – Toronto – Singapore, 1987).
63. S. P. Kuznetsov, *Dynamical Chaos* (Moscow, Fizmatlit, 2001). (In Russian.)



64. A. P. Kuznetsov, A. Yu. Kuznetsova, and I. R. Sataev, On critical behavior of a map with Neimark–Sacker bifurcation at destruction of the phase synchronization at the limit point of the Feigenbaum cascade, *Izvestija VUZov – Prikladnaja Nelineinaja Dinamika (Saratov)* **11**(1):12–18 (2003). (In Russian.)
65. P. Collet, P. Coulet, and C. Tresser, Scenarios under constraint, *J. Physique Lett.* **46**:L143–L147 (1985).
66. J. A. C. Gallas, Degenerate routes to chaos, *Phys. Rev. E* **48**:4156–4159 (1993).
67. B. Hu and J. M. Mao, Period doubling: Universality and critical-point order, *Phys. Rev. A* **25**:3259–3261 (1982).
68. B. Hu and I. I. Satija, A spectrum of universality classes in period-doubling and period tripling, *Phys. Lett. A* **98**:143–146 (1983).
69. P. R. Hauser, C. Tsallis, and E. M. F. Curado, Criticality of rouds to chaos of the  $1 - a|x|^2$ , *Phys. Rev. A* **30**:2074–2079 (1984).
70. D. V. Lubimov, A. S. Pikovsky, and M. A. Zaks, Universalities and scaling at the transition to chaos through homoclinic bifurcations, *Renormalization Group*, eds. D. V. Shirkov, D. I. Kazakov, and A. A. Vladimirov (World Scientific, Singapore, New Jersey, Hong Kong, 1988), pp. 278–289.
71. J.-M. Gambaudo, I. Procaccia, S. Thomae, and C. Tresser, New universal scenarios for the onset of chaos in Lorenz-type flows, *Phys. Rev. Lett.* **57**:925–928 (1986).
72. M. A. Zaks and D. V. Lubimov, Bifurcation sequences in the dissipative systems with saddle equilibria, *Dynamical Systems and Ergodic Theory* **23**:367–380. (Banach Center Publications, Warszawa, 1989).
73. J.-P. Eckmann and H. Epstein, Bounds on the unstable eigenvalue for period doubling, *Commun. Math. Phys.* **128**:427–435 (1990).
74. K. M. Briggs, T. W. Dixon, and G. Szekeres, Analytic solution of the Cvitanović–Feigenbaum and Feigenbaum–Kadanoff–Shenker equations, *Int. J. Bifurcation Chaos* **8**:347–357 (1998).
75. A. Arneodo, P. Coulet, and V. Tresser, A renormalization group with periodic behaviour, *Phys. Lett. A* **70**:74–76 (1979).
76. B. D. Mestel and A. H. Osbaldestin, Feigenbaum theory for unimodal maps with asymmetric critical point: rigorous results, *Commun. Math. Phys.* **197**:211–228 (1998).
77. B. D. Mestel, A. H. Osbaldestin, and A. V. Tsygvintsev, Bounds on the Unstable Eigenvalue for the Asymmetric Renormalization Operator for Period Doubling, *Commun. Math. Phys.* **250**:241–257 (2004).
78. R. V. Jensen and L. K. H. Ma, Nonuniversal behavior of asymmetric unimodal maps, *Phys. Rev. A* **31**:3993–3995 (1985).
79. B. E. Oldeman, B. Krauskopf, and A. R. Champneys, Death of period-doublings: locating the homoclinic-doubling cascade, *Physica D* **146**:100–120 (2000).
80. S.-J. Chang, M. Wortis, and J. A. Wright, Iterative properties of a one-dimensional quartic map: Critical lines and tricritical behavior, *Phys. Rev. A* **24**:2669–2684 (1981).
81. S. Fraser and R. Kapral, Universal vector scaling in one-dimensional maps, *Phys. Rev. A* **30**:1017–1025 (1984).
82. S. P. Kuznetsov, Tricriticality in two-dimensional maps, *Phys. Lett. A* **169**:438–444 (1992).
83. A. P. Kuznetsov, S. P. Kuznetsov, L. V. Turukina, and E. Mosekilde, Two-parameter analysis of the scaling behavior at the onset of chaos: Tricritical and pseudo-tricritical points, *Physica A* **300**:367–385 (2001).
84. R. S. MacKay and C. Tresser, Boundary of topological chaos for bimodal maps of the interval, *J. London Math. Soc.* **37**:164–181 (1988).

85. R.S. MacKay and J. B. J. van Zeijts, Period doubling for bimodal maps: a horseshoe for a renormalisation operator, *Nonlinearity* **1**:253–277 (1988).
86. A. P. Kuznetsov, S. P. Kuznetsov, and I. R. Sataev, From bimodal one-dimensional maps to Hénon-like two-dimensional maps: does quantitative universality survive? *Phys. Lett. A* **164**:413–421 (1994).
87. J. Carcasses, C. Mira, M. Bosch, C. Simo, and J. C. Tatjer, Crossroad area–spring area transition (I) Parameter plane representation, *Int. J. Bifurcation Chaos* **1**:183–196 (1991).
88. J. Milnor, Remarks on iterated cubic maps, *Experimental Mathematics* **1**:5–24 (1992).
89. B. R. Hunt, J. A. C. Gallas, C. Grebogi, J. A. Yorke, and H. Koçak, Bifurcation Rigidity, *Physica D* **129**:35–56 (1999).
90. A. P. Kuznetsov, S. P. Kuznetsov, and I. R. Sataev, Three-parameter scaling for one-dimensional maps, *Phys. Lett. A* **189**:367–373 (1994).
91. K. M. Briggs, G. R. W. Quispel, and C. J. Thompson, Feigenvalues for Mandelsets, *J. Physics A: Math. General* **24**:3363–3368 (1991).
92. K. M. Briggs, *Feigenbaum scaling in discrete dynamical systems*. PhD Dissertation (University of Melbourne, 1997).
93. S. P. Kuznetsov, Cascade of period doubling in complex cubic map, *Izvestija VUZov – Prikladnaja Nelineinaja Dinamika (Saratov)* **4**(1):3–12 (1996). (In Russian.)
94. A. I. Golberg, Ya. G. Sinai, and K. M. Khanin, Universal properties for the period-tripling bifurcations, *Uspekhi Matem. Nauk* **38**:159–160 (1983).
95. P. Cvitanović, J. Myrheim, Universality for period  $n$ -tupling in complex mappings *Phys. Lett. A* **94**:329–333 (1983).
96. B. B. Mandelbrot, On the quadratic mapping  $z \rightarrow z^2 - \mu$  for complex  $\mu$  and  $z$ : The fractal structure of its M set, and scaling, *Physica D* **7**:224–239 (1983).
97. O. B. Isaeva and S. P. Kuznetsov, On scaling properties of two-dimensional maps near the accumulation point of the period-tripling cascade, *Regular and Chaotic Dynamics* **5**:459–476 (2000).
98. J. M. Mao, I. I. Satija, and B. Hu, Period doubling in four-dimensional symplectic maps, *Phys. Rev. A* **34**:4325–4332 (1986).
99. A. Lahiri, Inverted period-doubling sequences in four-dimensional reversible maps and solutions to the renormalization equations, *Phys. Rev. A* **45**:757–762 (1992).
100. S. J. Shenker, Scaling behavior in a map of a circle onto itself: Empirical results, *Physica D* **5**:405–411 (1982).
101. M. J. Feigenbaum, L. P. Kadanoff, and S. J. Shenker, Quasiperiodicity in dissipative systems: A renormalization group analysis, *Physica D* **5**:370–386 (1982).
102. S. Ostlund, D. Rand, J. Sethna, and E. Siggia, Universal properties of the transition from quasi-periodicity to chaos in dissipative systems, *Physica D* **8**:303–342 (1983).
103. X. Wang, R. Mainieri, and J. H. Lowenstein, Circle-map scaling in a two-dimensional setting, *Phys. Rev. A* **40**:5382–5389 (1989).
104. J. Stavans, F. Heslot, and A. Libchaber, Fixed Winding Number and the Quasiperiodic Route to Chaos in a Convective Fluid, *Phys. Rev. Lett.* **55**:596–599 (1985).
105. M. Bauer, U. Krueger, and W. Martienssen, Experimental studies of mode-locking and circle maps in inductively shunted Josephson-junctions, *Europhysics Letters* **9**:191–196 (1989).
106. J. A. Gazier and A. Libchaber, Quasi-periodicity and dynamical systems – An experimentalists view, *IEEE Trans. Circuits Systems* **35**:790–809 (1988).
107. J. D. Farmer and I. I. Satija, Renormalization of the quasiperiodic transition to chaos for arbitrary winding numbers, *Phys. Rev. A* **31**:3520–3522 (1985).

108. M. A. Zaks and A. S. Pikovsky, Farey level separation in mode-locking structure of circle mappings, *Physica D* **59**:255–269 (1992).
109. J. A. Ketoja, Renormalization in a circle map with two inflection points, *Physica D* **55**:45–68 (1992).
110. H.-C. Tseng, M.-F. Tai, H.-J. Chen, P.-C. Li, C.-H. Chou, and C.-K. Hu, Some scaling behaviors in a circle map with two inflection points, *Int. J. Modern Phys. B* **13**:3149–3158 (1999).
111. R. Delbourgo and B. G. Kenny, Fractal dimension associated with a critical circle map with an arbitrary-order inflection point, *Phys. Rev. A* **42**:6230–6233 (1990).
112. S. J. Shenker and L. P. Kadanoff, Critical Behavior of a KAM Surface. I. Empirical Results, *J. Stat. Phys.* **27**:631–656 (1982).
113. L. P. Kadanoff, Scaling for a critical Kolmogorov-Arnold-Moser trajectory, *Phys. Rev. Lett. A* **47**:1641–1634 (1981).
114. R. S. MacKay, A renormalization approach to invariant circles in area-preserving maps, *Physica D* **7**:283–300 (1983).
115. M. Widom and L. P. Kadanoff, Renormalization group analysis of bifurcations in area-preserving maps, *Physica D* **5**:287–292 (1982).
116. J. Wilbrink, New fixed point of the renormalisation operator associated with the recurrence of invariant circles in generic Hamiltonian maps, *Nonlinearity* **16**:1565–1571 (2003).
117. D. Del-Castillo-Negrete, J. M. Greene, and P. J. Morrison, Renormalization and transition to chaos in area preserving nontwist maps, *Physica D* **100**:311–329 (1997).
118. J. M. Greene and J. Mao, Higher-order fixed points of the renormalisation operator for invariant circles, *Nonlinearity* **3**:69–78 (1990).
119. T. W. Dixon, T. Gherghetta, and B. G. Kenny, Universality in the quasiperiodic route to chaos, *CHAOS* **6**:32–42 (1996).
120. B. V. Chirikov and D. L. Shepelyansky, Chaos border and statistical anomalies, *Renormalization Group*, eds. D. V. Shirkov, D. I. Kazakov, and A. A. Vladimirov (World Scientific, Singapore, New Jersey, Hong Kong, 1988), pp. 221–250.
121. C. Grebogi, E. Ott, S. Pelikan, and J. A. Yorke, Strange attractors that are not chaotic, *Physica D* **13**:261–268 (1984).
122. S. P. Kuznetsov, A. S. Pikovsky, and U. Feudel, Birth of a strange nonchaotic attractor: A renormalization group analysis, *Phys. Rev. E* **51**:1629–1632 (1995).
123. S. Kuznetsov, U. Feudel, and A. Pikovsky, Renormalization group for scaling at the torus-doubling terminal point, *Phys. Rev. E* **57**:1585–1590 (1998).
124. S. P. Kuznetsov, E. Neumann, A. Pikovsky, and I. R. Sataev, Critical point of tori collision in quasiperiodically forced systems, *Phys. Rev. E* **62**:1995–2007 (2000).
125. S. P. Kuznetsov, Torus fractalization and intermittency, *Phys. Rev. E* **65**:066209 (2002).
126. Y. Pomeau and P. Manneville, Intermittent transition to turbulence in dissipative dynamical systems, *Commun. Math. Phys.* **74**:189–197 (1980).
127. B. Hu and J. Rudnik, Exact solution of the Feigenbaum renormalization group equations for intermittency, *Phys. Rev. Lett. A* **26**:3035–3036 (1982).
128. J. E. Hirsch, B. A. Huberman, and D. J. Scalapino, Theory of intermittency, *Phys. Rev. A* **25**:519–532 (1982).
129. B. Hu and J. Rudnik, Differential-equation approach to functional equations: exact solutions intermittency, *Phys. Rev. A* **34**:2453–2457 (1986).
130. I. Procaccia and H. Schuster, Functional renormalization-group theory of universal  $1/f$  noise in dynamical systems, *Phys. Rev. A* **28**:1210–1212 (1983).
131. A. B. Zisook, Intermittency in area-preserving mappings, *Phys. Rev. A* **25**:2289–2292 (1982).

132. A. B. Zisook and S. J. Shenker, Renormalization group for intermittency in area-preserving maps, *Phys. Rev. A* **25**:2824–2826 (1982).
133. A. B. Zisook, The Complete Set of Hamiltonian Intermittency Scaling Behaviors, *Commun. Math. Phys.* **96**:361–371 (1984).